Cranial orientation and the lateral semicircular canal in primates: implications for palaeobiological reconstructions and the evolution of locomotor repertoires.

DISSERTATION

Submitted to the Faculty of Science, University of Witwatersrand in fulfilment for the requirements for the degree of

MASTERS OF SCIENCE BY DISSERTATION

(PALAEONTOLOGY)

By Christopher Pestana

Student Number: 1713895

ORCID ID: http://orcid.org/0000-0003-4026-2665

Supervisors: Dr. Julien Benoit – Evolutionary Studies Institute, University of Witwatersrand, Johannesburg, South Africa

Prof. Amélie Beaudet – Laboratoire de Paléontologie, Évolution, Paléoécosystèmes et Paléoprimatologie (PALEVOPRIM), UMR 7262 CNRS & University of Poitiers

ACKNOWLEDGEMENTS **5**

ABSTRACT **6**

CHAPTER 1 - INTRODUCTION **7**

CHAPTER 2 – THE VESTIBULAR METHOD **9**

CHAPTER 3 - PRIMATE LOCOMOTION AND THE EVOLUTION OF BIPEDALISM **12**

3.1 -Hominins **12**

3.2- Cercopithecoidea **13**

3.3- Spatial constraints on the morphology of the bony labyrinth **16**

CHAPTER 4 – AIMS AND RATIONALE **16**

CHAPTER 5 - MATERIALS AND METHODS **18**

CHAPTER 6– RESULTS **25**

6.1-Preliminary correlations and model selection **25**

6.2 - Evolutionary models **29**

6.3 - Fossils **33**

CHAPTER 7 – DISCUSSION **48**

7.1 - Neutral head posture v.s lateral canal orientation **48**

7.2- Obligate terrestriality **50**

7.3 - Can Bipedalism be inferred from Lateral SSC orientation? **52**

7.4- Brain mass.....54

7.5 - Implications for fossil data and the evolution of hominin terrestralisation.56

7.6 - Potential drawbacks 56

CONCLUSION.....57

APPENDIX.....58

REFERENCES.....75

ACKNOWLEDGEMENTS

I would like to thank my supervisors Dr. Julien Benoit and Prof. Amélie Beaudet for their guidance throughout this project. I am grateful to Wits University for a Post- Graduate merit award, and to Dr. Julien Benoit ,Dr. Keniloe Molopanye and Dr. Lucinda Backwell for generous funds. I would like to thank the South African National Biodiversity Intitute, Dr, Arnold Kanengoni at the Johannesburg Zoological gardens, Tracy Rehse and Lufuno Netshifhefhe at the National Zoological gardens in Pretoria, and Kara Heynis and the Lory Park Zoo. This project was also made possible by Gabi Krüger and the Petoria Human Bone Collection, The Evolutionary Studies Institute at Wits, The Ditsong Natural History Museum in Pretoria for use of their specimens which were scanned by Prof. Amélie Beaudet.

Friends, Family and departmental colleagues who have assisted me either financially or materially include the following people; Ryan honeyball, Kelly Kropman, Gavin Pincus, Shaun Richards, Sharne Van Wyk, Tyrone Minaar, Martinus Van Tee, Aragorn Eloff, Prof. Chantelle van Heerden, Alienor Duhamel, Sonia Sequiera, Dr. Bonita Birch, Prof. Lee Berger, Dr. Tammy Reynhard, Dr. Jerome Reynhard, Ashleigh Pestana, Dominic Pestana, and the Pestana family in New Zealand. Special thanks to Dr. Berhard Zipfel for reading through and providing comments on a draft of this dissertation.

ABSTRACT

The lateral semicircular canal and its predicted relation to head posture have been used in reconstructions of locomotion and posture of contemporary and extinct species, and in the evolution of bipedalism. Inferences of head posture in fossil species sometimes assume that the lateral semicircular canal is held near the earth's horizontal when the head is at rest. Despite the physiological importance of the vestibular system, the relationship between head posture and lateral semicircular canal orientation in primates has not been explored on a statistically significant sample, using phylogenetically corrected methods. This study tests the hypothesised relationship between lateral semicircular canal orientation and head posture in primates, and investigates potential links to locomotor categories.

This study finds that lateral canal orientation is not significantly correlated to positional repertoires. Significant differences in canal orientation are detected between terrestrial and arboreal species. Neutral head posture distinguishes several locomotor categories, and explains a moderate proportion of the variance in positional behaviour. Brain mass is found to correlate with positional behaviour when correcting for the effects of the phylogeny. The implications of the evolution of head posture in fossil species are discussed.

CHAPTER 1 - INTRODUCTION

The vestibular system is crucial to autonomic behaviours, perception, orientation in space, stabilisation of gaze during head movements, and maintenance of balance (Purves et al., 2018). The sensory organs of the vestibular system are constituted by three semicircular canals (see figure 1.1) and the otolith organs, the former detects angular accelerations, while the latter detects linear accelerations (Cullen, 2012). Detection of head movements is facilitated by a combination of signals from the semicircular canals that communicate information along the axes of rotation in 3- dimensions (Luo, 2020). The vertical canals are involved in controlling balance, while the lateral canals are involved in navigation (Angelaki and Cullen, 2008). Opposite pairs of semicircular canals function in a push pull fashion: when one side is inhibited the other is excited (Graf, 1988; David et al., 2010). The lateral semicircular canals (Lateral SSC) are most affected during yaw movements when the visual field is rotated about the transverse plane (Blanks et al., 1975).

The angular velocity from the semicircular canals must be integrated with gravitational signals, which then undergo decomposition into components perpendicular and parallel to gravity (Angelaki and Cullen, 2008). Accurate motor control is achieved via differential processing between active and passive head movements (Angelaki and Cullen, 2008). The importance of the vestibular is underscored by instances where its absence results in severe vertigo, postural irregularities, and destabilisation of the visual field (Cullen, 2012).

For over a century authors have posited a functional relationship between the orientation of the semicircular canals and head posture (Girard, 1910, 1923, 1924, 1929; Perez, 1922; de Beer, 1947; Delattre and Anthony, 1951; Delattre and Fenart, 1957, 1958; Vidal et al., 1986; Spoor and Zonneveld, 1998c; Fitzpatrick et al., 2006; Hullar, 2006; Coutier et al.,

2017; Schellhorn, 2018; Le Maître, 2019). Physiological data show that changes in head posture change how signals communicated by the semicircular canal are interpreted by the brain (Fitzpatrick et al., 2006). To understand how these signals are transmitted, it has been recommended that the position of each canal in relation to the rest of the skull must be properly defined (Blanks et al., 1975).

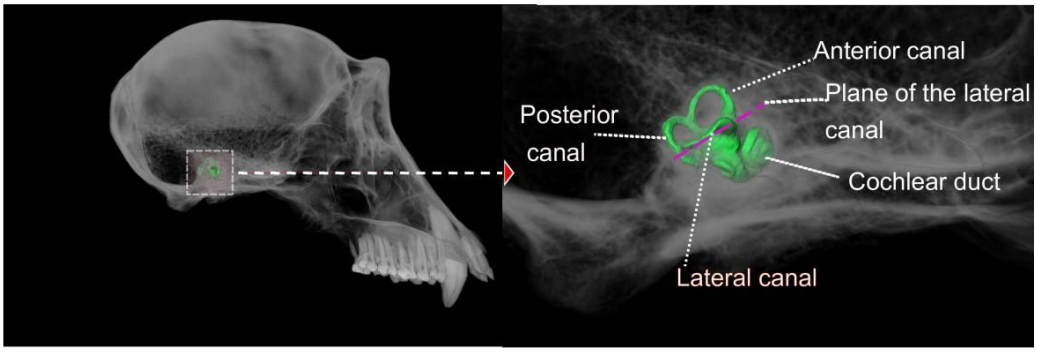

Figure 1.1: Right lateral view of *Gorrila gorilla* skull (left) with basic anatomy of the bony labyrinth labelled (right).

Palaeontologists, anatomists, and zoologists sometimes use the orientation of the lateral SCC of the inner ear to infer head posture of extinct species, assuming that its plane is almost horizontal when the animal holds its head in a relaxed or alert posture (Schoenemann, 1906; Benoit-Gonin and Lafite- Dupont, 1907; Lebedkin, 1924; Girard, 1929; Van Der Klaauw, 1952; Bull, 1969; Spoor and Zonneveld, 1998c; Spoor, 2003a; Hullar, 2006b; Witmer et al., 2008; Le Maître et al., 2017). However, controversy has long persisted over what planar system should be used to determine head posture in primates, especially when humans are included in the dataset (Anthony, 1953; Strait and Ross, 1999; Hullar, 2006).

Given that the lateral canal is more sensitive to rotational movements in the horizontal plane, a horizontal orientation of the plane of the lateral SCC has been justified on theoretical grounds (de Beer, 1947). It has been deduced that quadrupedal individuals hold their head higher than bipedal ones so that their eyes can face forward (Bullar et al., 2019). However, these hypotheses are not properly tested, and have been repeatedly challenged (de Beer, 1947; Blanks et al., 1975; Berlin et al., 2013; Marugán-Lobón et al., 2013; Benoit et al., 2020). They are also directly contradicted by some anecdotal observations which reported that if the lateral SCC of humans is aligned to the horizontal, the eyes are facing at a 20° - 30° angle below the horizontal (de Beer, 1947; Vidal et al., 1986b; Hullar, 2006; Taylor et al., 2009; Marugán-Lobón et al., 2013; Coutier et al., 2017; Schellhorn, 2018).

CHAPTER 2 – THE VESTIBULAR METHOD

Girard (1923) originally attempted to demonstrate that the lateral SCC aligned with earth's horizontal by dissecting the petrosals of a wide variety of animals and illustrating their skulls with their lateral SCC horizontally aligned (see figure 2.1) Given the physiological importance of the lateral SCC and presumed universality of the structures alignment to the horizontal, this led to a research tradition called the "vestibular method", which was argued to be superior to the Frankfurt plane due to properly accounting for anatomical and physiological properties (Delattre and Anthony, 1951; Anthony, 1953; Delattre and Fenart, 1957b, 1958). Since then, the lateral SCC has been argued to be an appropriate proxy for head posture across mammals, reptiles, and birds (Hullar, 2006). Despite a range of slight anterior tilts observed across taxa when comparing the orientation of the lateral SCC to earth's horizontal, Hullar (2006) argued that this standard was nonetheless consistent enough to merit its continued use.

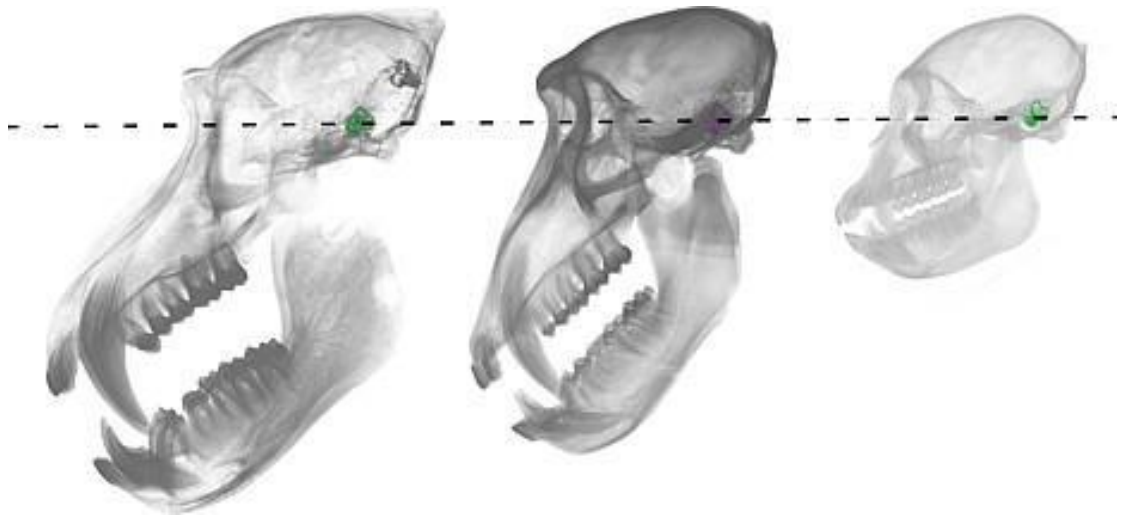

Fig 2.1: Cercopithecoid crania in left lateral view. From left to right : *Mandrillus sphinx, Papio ursinus, Lophocebus atterhimus.* Their heads are positioned with their lateral SCC's parallel to earth's horizontal plane following the vestibular method of Girard (1923).

Animals have also been theorised to align their lateral canals in parallel to the horizontal when alert (de Beer 1947). By photographing animals against a plumb line and then comparing these images to radiographs, de Beer (1947) inferred that animals held their heads with their lateral semicircular canals approximately horizontal, when in alert or habitual postures. However, when testing the hypothesis in humans, in a neutral poise, their lateral semicircular canals were estimated to tilt at an angle of between 24º and 37º.

It was reasoned that the orientation of the foramen magnum directs an anthropoids gaze forwards and downwards, and that it was possible that modern humans retained an anthropoid ancestral condition in the plane of the lateral semicircular canal (Beer, 1947) This could be related to spatial constraints of the vestibular-ocular reflex, or selection for the stability of the planar orientation of the canals (Spoor and Zonneveld, 1998). Still today, it

remains unclear as to whether de Beer was correct about the conservation of an anthropoid condition.

Macaques and squirrel monkeys, for instance, are reported to exhibit an angle of 10 degrees between the horizontal and the plane of the lateral semicircular canal (Blanks et al., 1985). Based on video footage shot against a plumb line, it was estimated that squirrel monkeys and crab-eating macaques held their lateral SCC's anteriorly tilted at an angle of 18 degrees from earth's horizontal, and that humans held their heads at 16 degrees from the horizontal at rest (Graf et al., 1995). Other research reports that the lateral SCC in humans is tilted at 5 degrees from the horizontal and that a similar tilt characterises non-human primates and other mammals (Vidal et al., 1986).

In contrast to other species, Girard (1923) originally proposed that the planes of the lateral semicircular canal in humans would be horizontal if a person directed their gaze 1 – 2m downwards in front of them. It was reasoned that during human bipedal locomotion the subject would benefit from such a head posture which would enable scanning irregularities on the ground, thereby optimising balance of multiple joints over a restricted surface area (Jaanusson, 1987). Other researchers have suggested that this possibility ought to be explored in the context of active locomotor states in humans specifically (Lieberman, 2011), and other primates more generally (Urciuoli et al., 2020). While these tests are beyond the scope of this study, testing if any relationship is apparent in resting and alert states would help supporting or ruling out this idea, directing researchers attention to more innovative thinking.

CHAPTER 3 - PRIMATE LOCOMOTION AND THE EVOLUTION OF BIPEDALISM

Reconstructing locomotor repertoire in fossil species is complicated by the paucity of post-cranial remains and footprints (rev. in Le Maître et al., 2017, but see McPhee 2018 for reconstruction of locomotion in sauropodomorphs). Indices of bipedalism recover conflicting phylogenetic signals, and there is still substantial debate on the nature of the evolutionary and developmental factors involved (eg. Young et al 2005; Young et al., 2008; di Vicenzo et al., 2008; Mongle et al., 2018; Landi et al., 2019; Prang, 2019). Drawing inferences about arboreality based on post-cranial morphologies alone should therefore be done with caution. Information from the semicircular canals can be used to complement and test locomotor reconstructions based on post- cranial remains, and provides a potential source of evidence in the absence of postcranial remains (Walker et al., 2008).

3.1 -Hominins

Bipedal posture and locomotion are an important hominin adaptation that has shaped human evolution (Day and Wickens, 1980; McHenry, 1982; Plomp et al., 2020; Raichlen and Pontzer, 2021; Marino et al., 2022). Australopithecus species are widely recognized as bipeds (Lovejoy et al., 1973; Lovejoy, 1975; Day and Wickens, 1980; White, 1980; McHenry, 1982; Latimer and Lovejoy, 1989; Ward, 2013; Williams et al., 2021). However, whether all Australopithecus species shared equivalent proportions of arboreal and terrestrial behaviours in their positional repertoire remains unresolved (Ward, 2013)

Research on hominin feet suggests that there existed a diversity in bipedal abilities among early hominins (e.g. Zipfel et al., 2011; DeSilva et al., 2013; McNutt et al., 2018). Evidence from foot morphology of Australopithecus suggests that these species display a mosaic of primitive and derived characteristics (e.g. Zipfel et al., 2011; DeSilva et al., 2013). Alternatively, some of these characters could be examples of intraspecific variation shared among Australopithecus species (e.g. Boyle et al., 2018). *Australopithecus africanus*, a species considered in the present study, evinces a human-like loading pattern of the hip (Ryan et al., 2018; Georgiou et al., 2020).

The Laetoli footprints suggest that the most probable species to have made them had a gait that was different from both Pan and modern Homo (Hatala et al., 2016). A.L. 288-2-1, a specimen attributed to *Australopithecus afarensis*, has been noted to showcase longer humeri than femori and diaphyseal strength better approximates a great ape condition (Ruff et al., 2016). Comparisons between Australopithecus species has suggested that limb proportions in *Australopithecus africanus* to be more similar to great apes, while *Australopithecus afarensis* was more human-like (e.g. McHenry and Berger, 1998 ; Green et al., 2007). Furthermore, semicircular canal radii and size have previously been suggested to indicate that Australopithecus species (including Sts 5) were more facultative bipeds rather than obligate bipeds with a repertoire that included substantial swinging (Spoor et al., 1994; Spoor and Zonneveld, 1997). A recent study found that some southern African Australopithecus share aspects of their vestibular system with chimpanzees while others are more similar to humans (Beaudet et al., 2019).

3.2- Cercopithecoidea

Aside from *Homo sapiens*, baboons are the primates most widely (in the biogeographic sense) adapted to a terrestrial existence, providing good comparative examples of challenges of the landscape faced by our forebears (DeVore and Washburn, 1963). More generally, cercopithecoids are a useful control group for uncovering evolutionary patterns and adaptations of early hominins, given they are the most closely related group to hominins after the great apes (Beaudet et al., 2016). The primitive condition of stem cercopithecoids is still debated, some suggesting that they are primitively arboreal (Napier, 1970; Rollinson, 1981; Frost and Delson, 2002), and others suggesting a semi-terrestrial repertoire (Strasser, 1988; Ciochon, 1993). Under traditional discriminant function analysis, Cercopithecoid semicircular variation is an unreliable diagnostic of taxonomic affiliation; however, they are reliable in detecting morphological affinities that may be a product functional signals that are under the control of locomotor activity (Beaudet et al., 2016).

Cercopithecoids also serve as an important proxy for palaeoenvironmental reconstruction throughout the Plio-Pleistocene (Carter, 2006; Deane et al., 2022). This is in part due to their widespread geographic occurrence and occupation of multiple niches through-out this period. This widespread geographic range has been used to link changes between East African and southern African sites (Gilbert et al., 2016). Besides the work by Beaudet (2015), Beaudet et al. (2016), and Thackeray et al. (2019), little has been done to understand the relevance of the bony labyrinth of Plio-Pleistocene fossil cercopithecoids. Furthermore, no work to date has attempted to estimate head posture or explore the potential association between lateral canal orientation, locomotion and palaeoenvironment in Primates.

Fossil cercopithecoids considered in this study - *Cercopithecoides williamsi*, *Parapapio whitei*, *Parapapio jonesi*, *Dinopithecus ingens* and *Papio angusticeps*, are Plio-

Pleistocene primates that occur in many of the same deposits as *Australopithecus* species (Maier, 1977; Berger et al., 2002; Williams et al., 2007; Pregibon and Williams, 2021; Beaudet, 2023). *Cercopithecoides williamsi*, an extinct colobine, has variously been considered to be highly terrestrial (Birchette, 1982), or adapted to an open mixed habitat (Elton, 2000). One carbon isotope study showed that there were differing signals between specimens with some specimens reflecting a mixed terrestrial/arboreal diet and others a wholly terrestrial diet (Fourie et al., 2008). *Papio angusticeps* is a basal baboon species (Adams and Rovinsky, 2018), whose incidence in the fossil record coincides with molecular dates of the earliest divergence estimates for modern baboons (Gilbert et al., 2015). Predicting the neutral head posture of this species would be important to understanding the evolutionary pathways of head posture and how they have changed with respect to the basal condition.

Elton (2001) pointed out that many of the postcranial elements found in Sterkfontein member 4 and Bolt's farm were indicative of a forested arboreal habitat. This evidence was used to suggest the possibility that at least some members of *Parapapio* were forest dwellers. Palaeobotanical work suggests that the deposits from Sterkfontein member 4 comprised a partially forested habitat (Bamford, 1999). This could be consistent with *Australopithecus africanus* exhibiting some arboreal locomotion as part of its repertoire. However, it is important to note that the mere presence of a woodland habitat in the palaeoecological record does not entail that a specific taxon inhabited this habitat (Faith et al., 2021). Inferences from lateral SCC orientation may help to clarify the behavioural ecology of these primates.

3.3- Spatial constraints on the morphology of the bony labyrinth

Changes in semicircular canal morphology in hominins can also be a consequence of spatial limitations brought about by changes in the size and organisation of the brain and constraints of the basicranium (spatial packing hypothesis) (Biegert, 1957). Labyrinthine morphology remains partially liable to transformations in shape of surrounding structures during prenatal development (Delattre and Fenart, 1960, 1961, 1962; Spoor and Zonneveld, 1998; Malinzak, 2010; Lebrun et al, 2012; Le Maitre et al., 2017). For instance, changes in the position of the lateral canals have been proposed to be linked to the rotation of the petrosals (Delattre and Fenart, 1958, 1961, 1962), which in turn has been linked to cranial flexion and/or encephalization (Dean, 1988), and semicircular radii have been shown to be significantly correlated with brain size in primates (Malinzak, 2010). This is why interactions between brain size and lateral canal orientation are investigated here too along with lateral SCC orientation. Research in archosaurs (Benson et al., 2017, Bronzatti et al., 2021), and turtles (Evers et at., 2022) has recently added support to the spatial packing hypothesis, and have shown ecological signals based on labyrinthine morphology to be inconsistent.

CHAPTER 4 – AIMS AND RATIONALE

The orientation of the lateral semicircular canal has historically been used to infer locomotor repertoire in primates (Malinzak et al., 2012a; Ryan et al., 2012), bipedalism in hominins (Spoor et al., 1994; Spoor and Zonneveld, 1998a; Spoor, 2003a; Le Maître, 2019), as well as locomotor behaviours in various other extant and extinct species (Witmer et al., 2008;

Bullar et al., 2019; Schade et al., 2020). However, this assumption has seldom been tested in a statistically significant and phylogenetically corrected framework, and anecdotal evidence strongly argues against its veracity (deBeer 1947).

The current state of knowledge calls for a critical reappraisal of the hypothesis that the lateral SCC can be used as a reliable proxy to infer head posture at rest in primates. Such a comparative study has yet to be conducted. The present study addresses this hypothesis on Primates at a broad taxonomic scale, and using a statistical approach that includes phylogenetic comparative methods (PCM's). Predictions from this study can be used to reconstruct head posture and infer the ecological preferences and locomotor modes in extinct primates.

This study is an inquiry into the status of lateral semicircular canal orientation as a reliable proxy for the reconstruction of head posture and locomotor repertoires in primates, and asks if a statistically significant correlation between reconstructed postures and earth's horizontal plane holds among primates. The following main hypotheses are proposed:

1) The orientation of the LSCC aligns with earth's horizontal plane when a primate adopts a neutral head posture.

2) Neutral head posture is significantly correlated with LSCC orientation.

3) Neutral head postures can be used to predict locomotory behaviour.

4) Brain mass can be used to predict LSCC orientation.

5) Brain mass can be used to predict Neutral head posture.

The final goal of this project was to statistically determine, using modern primates, whether using the lateral semicircular canal is a valid approach to reconstruct head posture and bipedalism in extinct hominins. If successful, postural and locomotor repertoires of extinct primates could be reconstructed from canal orientation. If no significant correlation is found between the lateral semicircular canal orientation and that of the head is not significant, then this will statistically invalidate a long-held belief in palaeontology, and implications will have to be discussed. More particularly, the impact of the size and reorganisation of the brain (the cranial integration hypothesis) will be one of the avenues to be explored to account for this result.

CHAPTER 5 - MATERIALS AND METHODS

This study followed the methodology outlined in Benoit et al. (2020). CT scans of a sample of 73 extant primate skulls covering 27 species were obtained from the open-access database Morphosource (Boyer et al., 2016), the University of Kyoto digital primatology museum and from the European Synchrotron Facilities vertebrate biology collection (http://paleo.esrf.eu/index.php?/category/1783).

Scans of modern human skulls were obtained with permission from the Pretoria Bone Collection at the Department of Anatomy of the University of Pretoria. Scans of , Sts 565 (*Parapapio jones*i), MP 221 (*Parapapio whitei*), and KA 194 *(Papio angusticeps),* were obtained with permission from the Ditsong National Museum of Natural History Collection. Scans of Sts 5, (*Australopithecus africanus),* and MP3a (*Cercopithecoides williamsi*) were obtained from the Evolutionary Studies Institute at Wits University in Johannesburg. Specimens obtained from morphosource https://www.morphosource.org/ are housed at the following institutions: Kyoto university, Museum of comparative zoology, Harvard

university, The American Museum of Natural history, European synchrotron research facility, Institut des Sciences de l'Evolution den Montpellier, Stony Brook University, Southern Illinois University, and Duke University Lemur Centre. All cranial specimens used in this study along with their institutional abbreviations and accession numbers are listed in Appendix (Table 1).

To establish the actual resting head posture in the corresponding primate species, photos were taken at the Johannesburg and Pretoria National zoological gardens, and the Lory park (Midrand). To ensure that earth's horizon was parallel with the long borders of the photograph, a spirit level was attached to the camera (Canon powershot SX60 HS). Animals were photographed in lateral position when the spirit level was calibrated with all bubbles properly aligned, thereby obtaining the desired orientation.

Zoos were deemed appropriate environments to take photographs as the animals are accustomed to human presence. A waiver for photographing the specimens was obtained from Wits animal ethics committee (Waiver 26-05-21-O), and permission was obtained from the zoos. A medical ethical clearance certificate (M220381) was obtained from the Wits medical ethics committee to digitally reconstruct human bony labyrinths, and to photograph volunteers drawn from the scientific community at the Evolutionary Studies Institute (ESI). Photograph measurements are listed in Appendix (Table 2).

Measurements of the angle between the horizontal axis and a modification of the Frankfurt horizontal on the photos were performed using the software Image J (Rasband, 1997) (see figure 5.1, left column). Measurements done parallel to the borders of the photograph (see red dashed line on figure 5.1). Holding shift while taking a measurement on Image J results

in line parallel with the long borders of the image (Ferreira and Rasband, 2012). Figures ensure their equivalence to earth's horizontal plane. The modified Frankfurt horizontal is defined here as a line connecting the ventral most point of the orbit (orbitale) to the superior most point on the external auditory meatus (porion). Since the traditional Frankfurt horizontal only orients the skull in left lateral view using the left porion (White et al., 2012), the modified definition is used so that measurements could be obtained on both sides of the head with porion points on both right and left orbitals used (Freimann et al (2014). To correct for intra-observer error measurements were done 3 times and values greater than 3 standard deviations of the which are flagged in table 1, were excluded from the analyses.

The bony labyrinths were manually segmented from the CT scans at the virtual imaging palaeontology lab of the Evolutionary Studies Institute using the software Avizo 9 (VSG, Hillsborough, USA). Head posture was reconstructed in the same software, using the lateral semicircular canal as a baseline (as per the literature). The angle was calculated by comparing the plane of the lateral semicircular canal to the Frankfurt horizontal (see figure 5.1) Coefficients of from the standard deviation for labyrinthine angles was calculated by taking 10 measurements (5 on each ear) from 2 specimens, see Appendix table 4

Statistical comparisons were then made between the reconstructed posture using lateral SSC orientation and the actual head posture of specimens in R- statistical software version 4.2.2 (R Core Team, 2022). Preliminary correlations between variables in the dataset were assessed using the 'ggpairs' function in the 'Ggally' package (Schloerke et al., 2021). The function computes and charts Pearson correlations with significance levels across multiple pairs of variables. The preliminary analysis included neutral head postures, brain mass, body mass, locomotor diversity indices, primary locomotor category and substrate use.

Data on brain mass and body mass for extant species was obtained from (Isler et al., 2008a), and locomotor categories (bipedalism, brachiation, terrestrial quadrupedalism, arboreal quadrupedalism, and vertical climbing), and diversity indices are from (Granatosky, 2018), which contained the most comprehensive data on standardised positional repertoires following (Hunt et al., 1996) to date. Data for endocranial volume (ECV) of fossil cercopithecoids was obtained from (Beaudet et al., 2016b), and converted using the formula from $1.147 \times (\text{ECV})^{0.976}$ (Ruff et al., 1997). Brain mass data for *Australopithecus africanus* was obtained from (de Sousa and Cunha, 2012), and data for *Gorilla gorilla* was taken from (Montgomery, 2018). All values were transformed using a natural logarithm (see Appendix table 3). Logging variables was done to bring values closer to linearity, normality and homoscedasticity.

The locomotor diversity indices from Granotsky are based on measures taken from the Shannon Weaver diversity index (Shannon, 1949), and applied to standardised positional behaviour. They are denoted by the equation: ¼ ∑ pi ln pi, where pi is the proportion of a particular locomotor behavior divided by the sum of all locomotor behaviours. Correlations were then checked by subjecting ordinary least squares analysis to model fits tests using the base ANOVA function in R to assess if interactions, co-predictors, and models besides the main one where neutral head posture is predicted from reconstructions, could provide better predictions for neutral head posture in fossil specimens

A phylogenetic approach was considered important to performing analysis on aspects of the bony labyrinth, since vestibular morphology has been demonstrated to have a high

phylogenetic signal (Lebrun et al., 2010; Benoit et al., 2020; Urciuoli, 2021). A phylogenetic tree was estimated using nucleotide sequences from 10k trees website (Arnold et al., 2010), while morphological data for cercopithecoids was obtained from Pugh and Gilbert (2018. suppl). Morphological data for great ape species, *Australopithecus africanus,* and modern humans was taken from Dembo et al. (2016. suppl). Nucleotide sequences were aligned using Clustal X (Jeanmougin et al., 1998), and a rate model for each sequence were selected using the stochastic IQ- tree algorithm (Nguyen et al., 2015).

The phylogenetic tree was then inferred under a total evidence approach in the software MrBayes 3.2.6 (Ronquist et al., 2012). Branch length priors were set to a fossilised birth death prior, with a sampling probability of 1, and a diversity sampling strategy. The speciation prior was set to exponential 1 and the extinction prior was set to a beta distribution of (1, 1). The clock rate prior was set to a lognormal distribution (0, 1). Topological constraints on clades consistent with the literature were assigned to the root. These were hominins, hominoids, guenons, cercopithecoids, papionins, lemuroids and mandrills. 4 markov chains were run with a diagonal sampling frequency of 1000, at a temperature of 0.3, and a burn in fraction of 0.50 was discarded. A total of 60 0000 generations were sampled and all compatible trees were summarised to obtain the final tree. Convergence of samples was assessed by assessing that all standard deviations of split frequencies were under 0.01, and then chains were also checked visually in Tracer (Rimbaut et al., 2018). Since the character matrices used did not include *Cercopithecus williamsi,* the taxon was grafted onto the tree using the 'bind.tree' function from the ape package (Paradis et al., 2004). The placement of *C. williamsi* alongside *Colobus guereza* is consistent with the consensus that they are colobine monkeys (Leakey 1982, Frost & Delson 2002, Frost et al., 2015). The tree is broadly consistent with recent studies on primates (e.g. Chattergee et al., 2009, Vanderpool et al., 2020). One notable difference, however, is that *Cercopithecus ascanius* and *Cercopithecus*

mona branch earlier than *Cercopithecus neglectus*. The misspecification of branch lengths however does little to affect the robustness in the application of phylogenetic comparative methods (Stone, 2011).

Statistical analyses such as phylogenetic least squares regression (PGLS) were carried out using the package 'nlme' (Pinheiro et al., 2017), and 'phylolm' (Tung Ho and Ané, 2014), the statistical software R version 4.2.2 (R-Core team 2022). Phylolm was used to obtain the R-squared values and in cases where there were problems with convergence in using nlme. Phylolm was favoured as the function easily permits adjustment of upper and lower bound of parameter. Evolutionary models tested included brownian motion (BM), l's lambda (λ), early burst (EB), and ornstein uhlenbeck (OU). Pagels's (1999) lambda measures phylogenetic signal in characters while simultaneously estimating the parameter, at $\lambda = 1$, the model is equivalent to brownian motion and at 0 the parameter is a star-phylogeny.

All data were log transformed prior to analysis to reduce skew in the datasets, reduce heteroscedasticity, and improve linearity. Non-normality is known to reduce statistical power (Mundry et al., 2014), while heteroscedasticity introduces measurement bias when relevant variables statistical contribution goes undetected (Graf and Hails 2002). Log-transforms are one way to correct this bias (Graf and Hails 2002). Lilliefors tests using the 'nortest' package were used to assess if residuals were approximately normally distributed (Gross et al., 2015).

Lilliefors test rejects the hypothesis of non-normality of the residuals at $\alpha <= 0.05$. When non-normality was detected due to outliers inter-specific regressions at across ecological

groups and at clade levels were conducted to test if these procedures could yield better predictions that do not violate model assumptions of phylogenetic general linear models, since different slopes could be evident at different groups in the phylogenetic tree (Yapuncich and Boyer, 2014; Smaers and Rohlf, 2016; Sansalone et al., 2020; Smaers et al., 2021; Gavrilov et al., 2022).

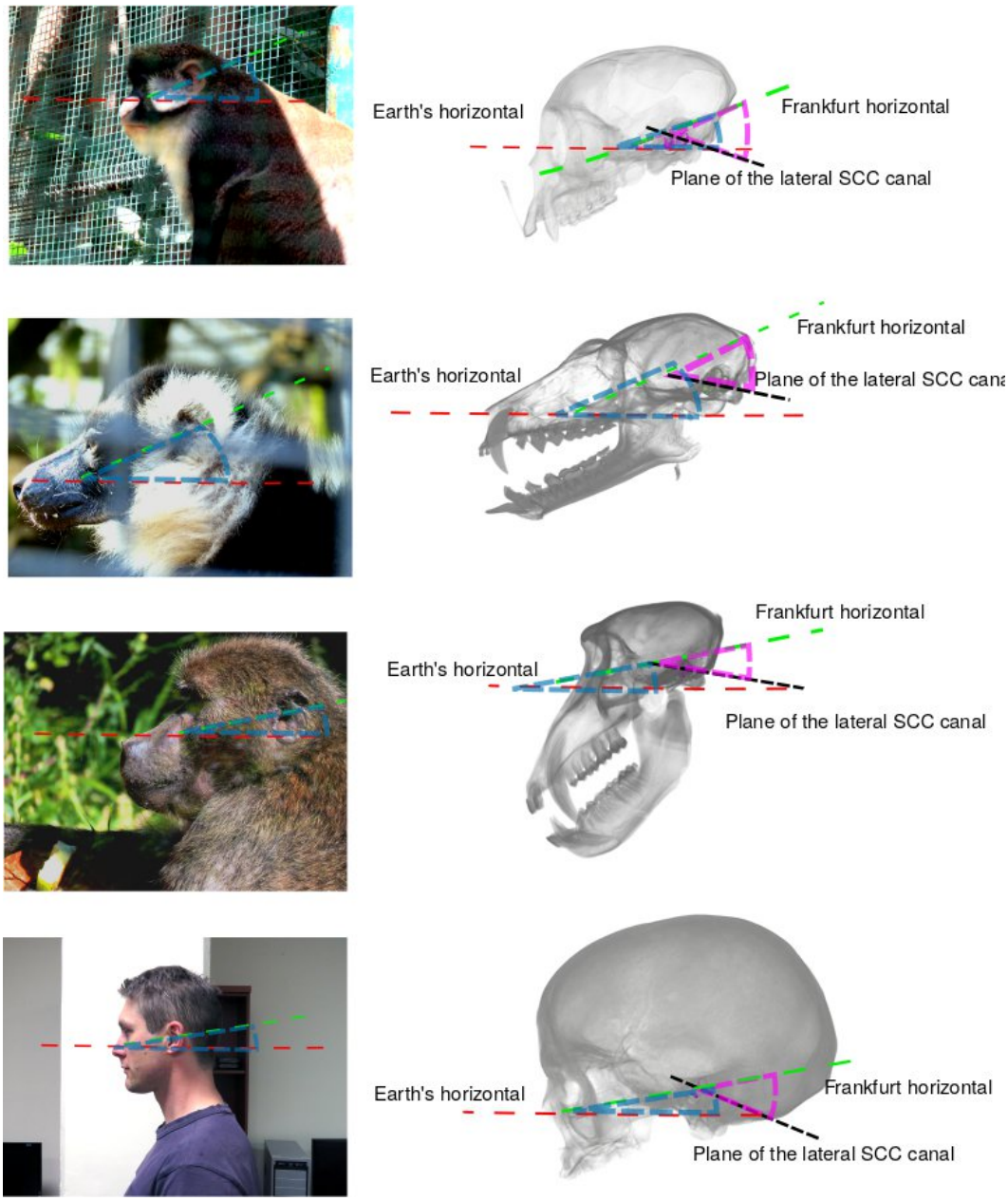

Fig 5.1: Images of primates from top: *Cercopithecus ascanius, Varecia variegata, Papio ursinus, and Homo sapiens*, adopting a neutral poise alongside crania of comparing Neutral head posture (blue angle) to lateral SCC orientation(pink angle).

Non phylogenetic models were diagnosed for heteroskedasticity using a Brasch-pagan test (Breusch and Pagan, 1979). Heteroskedasticity for the phylogenetic models was diagnosed using residual plots. model at $\alpha <= 0.05$. Heteroskedasticity is known to inflate type 1 error rates (Yang et al., 2019), and should therefore be diagnosed before performing phylogenetic linear regressions (Mundry et al., 2014). The most statistically stable models were used for predictions. Sub-setting for plots was done using code modified from Bertrand et al (2021 suppl), and the 'ggplot' package (Wickham et al., 2016) was used to create graphs.

CHAPTER 6– RESULTS

6.1-Preliminary correlations and model selection

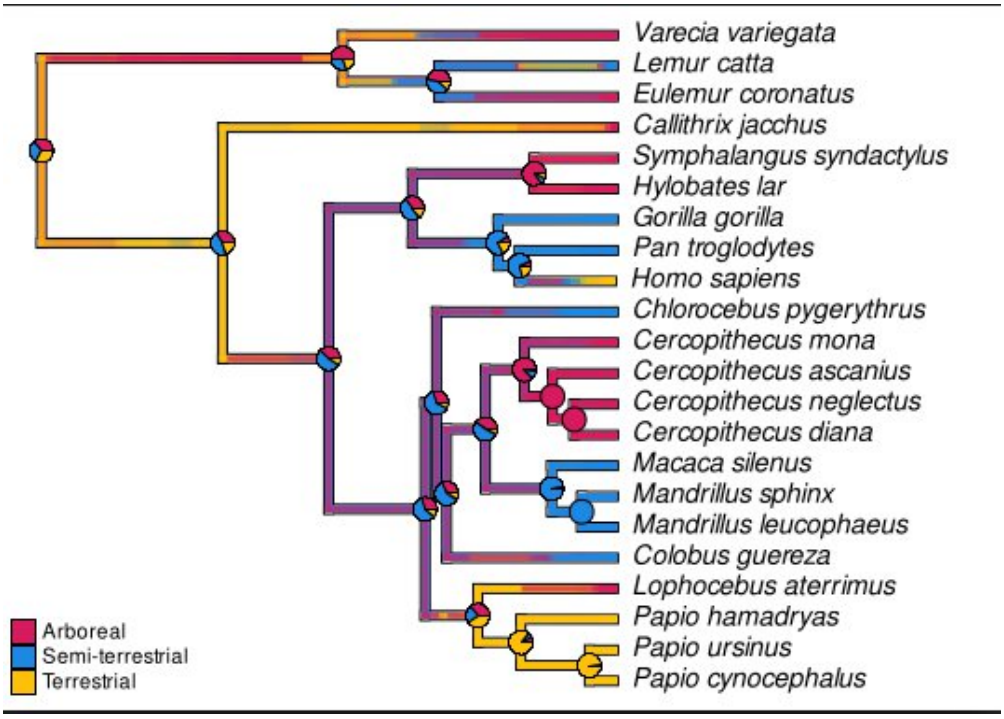

Figure 6.1.1: phylogenetic tree of extant species considered in this study with discrete character states (arboreal, semi-terrestrial, terrestrial) mapped using corHMM (Beaulieu et al., 2017), and phytools (Revell, 2012).

Preliminary Pearson correlations (Fig 6.1.1) of dataset including fossil data reveals no significant correlations between lateral canal orientation (LCO) and any of the variables in this subset of the data Locomotor mode is best correlated with body mass and brain mass with a coefficient of r=- 0.838 at α =0.001. Pearson's correlations do not recover significant correlations between neutral head posture and locomotion. These correlations are not phylogenetically corrected nor evaluated for model assumptions.

After analysing the models in Table 6.1.1, brain mass treated as an interacting variable with reconstructed lateral canal orientation to predict neutral head posture under a least squares model yields the lowest, and therefore, best fitting Akaike information criterion (AIC) and Bayesian information criterion score (BIC). However, when regressing the interaction the lines do not fit on the graph due to extreme intercept values, suggesting a problem with model structure due to the heteroskedasticity (see Table 6.1.3), and non-linear distribution of the variables.

The results of the computed effect sizes (Table 6.1.2) from the models show that brain mass has the highest effect size on the model. Lateral SCC orientation has a low, insignificant effect size, and body mass has a low significant effect. When testing whether reconstructed canal orientation was homoscedastic, the model fails this assumption (Table 6.1.3). When attempting to plot the model that treats brain mass as interacting

with canal orientation, the lines do not show on the plot due to the position of the intercepts, suggesting that the model fit is not linear.

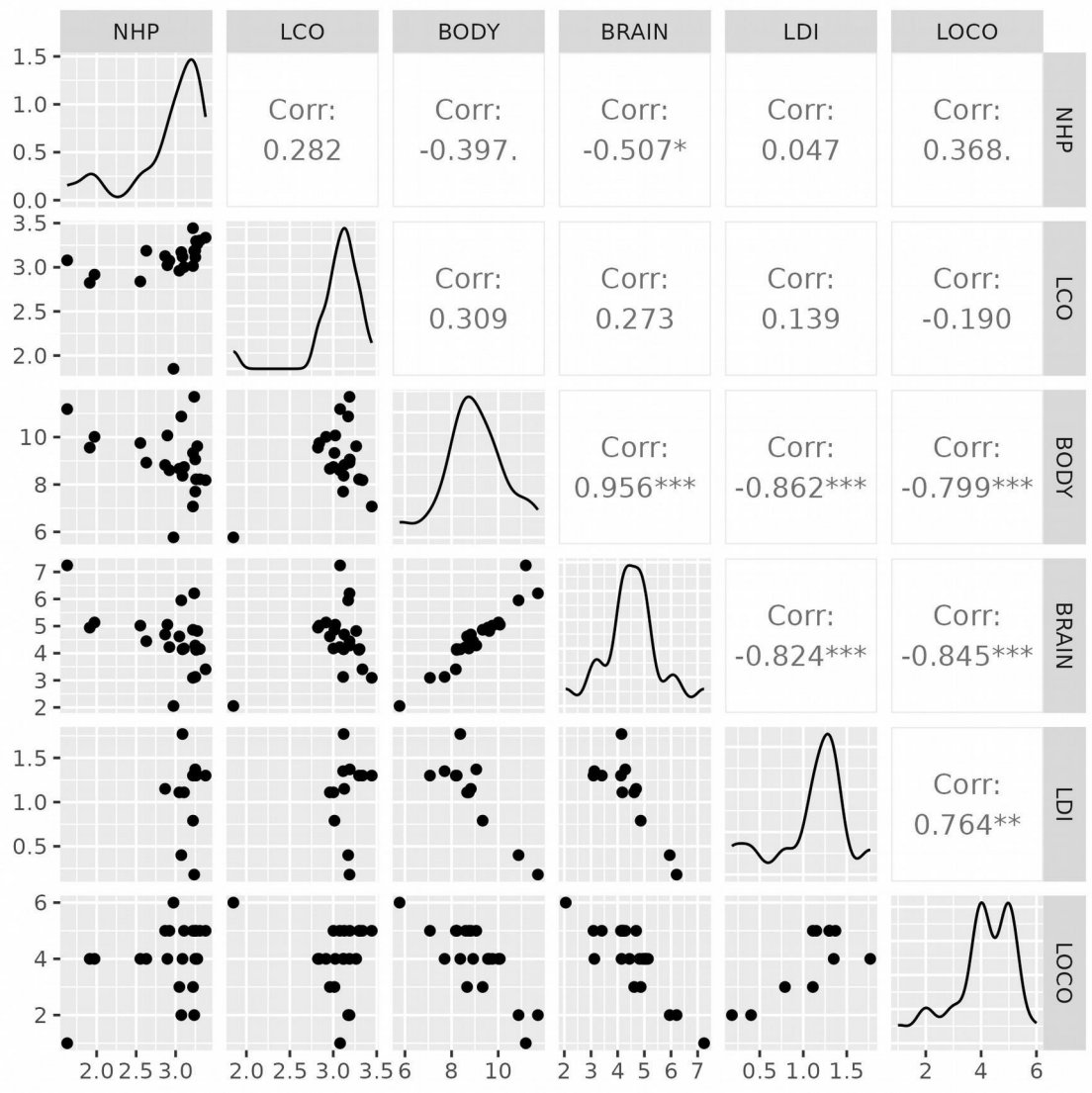

Fig 6.1.2: Pearson's preliminary (non-phylogenetically corrected) correlations across the dataset of extant species. Abbreviations are as follows: Neutral Head Postures (NHP), Lateral canal Orientation (LCO), Brain mass (BRAIN), Body mass (BODY) , Locomotor Diversity Index (LDI) * = significant at $\alpha < 0.05$, **, Locomotor mode= (LOCO). significant at $\alpha < 0.01$, *** significant at $\alpha = 0.001$. The variables best correlated with Locomotion and head posture are Brain mass and Body mass. These variables also correlate well with the Locomotor diversity Index.

Table 6.1.1: Comparison of model fits of ordinary least squares models (OLS) using AIC. The main model Neutral head postures~Lateral canal orientation has the least predictive value of all models. AIC = Akaike information criterion, BIC = Bayesian information criterion, LL = Log likelihood, LR = likelihood ratio.

OLS Model		AIC	BIC	LL	Test	LR	p-value
Neutral head postures ~ Lateral canal orientation	1	34.08	37.35	-14.04			
Neutral head postures ~ Lateral canal orientation+Brain mass	2	24.86	29.22	-8.43	1 vs 2	11.22	0.0008
Neutral head postures ~Lateral canal orientation×Brain mass	3	20.06	25.52	-5.03	2 vs 3	6.80	0.0091
Neutral head postures ~Brain mass	4		32.63	-11.68	3 v.s 4	13.30	0.0013
Neutral head postures~Brain mass + Body mass	5	24.61	30	8.78	4 vs 5	8.78	0.0126

Table 6.1.2: Computations of effect sizes for ordinary least squares models.

Response	Sum Sq	Df	F-value	Pr(>F)
(Intercept)	0.957	1	9.61	0.00651
Lateral canal orientation	0.288	1	2.89	0.107
Brain mass	1.275	1	12.80	0.00232

Body mass	0.341	1	3.43	0.0814
Lateral canal orientation :Brain mass	0.810	1	8.13	0.0111

Table 6.1.3: Breusch Pagan tests for heterosckedacity in the Ordinary least squares models The only model which does not show evidence of heteroskedacity is the the first model Neutral head postures vs lateral canal orientation. * = significant at $\alpha < 0.05$.

OLS Model	Breusch-Pagan test	df	p-value
Neutral head postures ~ Lateral canal orientation	1.1173	1	0.2905
Neutral head postures ~Lateral canal orientation*Brain mass	9.5628	3	0.02267*
Neutral head postures ~ Lateral canal orientation+Brain mass	7.9075	2	0.01918*
Neutral head postures ~ Brain mass	4.7372	1	0.02952*

6.2 - Evolutionary models

Table 6.2.1: Model selection table for evolutionary models of neutral head postures ~ lateral SCC orientation. Pagel is recovered as the best fitting according to AIC. The p-value also suggests a better model fit. Pagel has the lowest AIC value, as well as an improved model fit given the p-value. * denotes statistical significance at $\alpha <= 0.001$.

EB (Early Burst), OU (Ornstein Uhlenbeck), BROWNIAN (Brownian motion), PAGEL (Pagel's lambda). Df (degrees of freedom, AIC (Akaike information criterion), BIC (Bayesian information criterion), LL (Log-likelihood), LR (Likelihood ratio).

Model	Df	AIC	BIC	LL	LR	p-value
EB ln (Neutral head postures) ~ ln(LSCC orientation)	1	42.573	47.41	-19.069		

OU ln (Neutral head postures) ~ ln(LSCC orientation)	2	34.06	37.33	-14.03		
BM ln (Neutral head postures) ~ ln(LSCC orientation)	3	41.15	44.43	-17.254		
PAGEL ln (Neutral head postures) ~ ln(LSCC orientation)	4	25.86	30.22	1.339	39.1854	p<.0001**

Table 6.2.2: Model selection table for neutral head postures ~ brain mass. Pagel is the best fitting model. * denotes statistical significance at α </= 0.01. EB (Early Burst), OU (Ornstein Uhlenbeck), BROWNIAN (Brownian motion), PAGEL (Pagel's lambda).

Df (degrees of freedom, AIC (Akaike information criterion), BIC (Bayesian information criterion), LL (Log-likelhood), LR (Likelihood ratio).

Model	df	AIC	BIC	LL	Test	LR	p-value
EB ln(Neutral head postures) ~ ln(brain) mass	2	38.10	41.38	-16.05			
OU ln(Neutral head postures) ~ ln(brain) mass	3	29.35	32.63	-11.68			
BROWNIAN ln(Neutral head postures) ~ ln(brain) mass	4	36.86	40.14	-15.43			
PAGEL ln(Neutral head postures) ~ ln(brain) mass	5	5.04	9.40	1.48	4 vs 5	33.83	p<.0001*

Table 6.2.3: Lilliefors test for normality on the best fitting evolutionary models for Neutral head postures ~ Lateral canal orientation and Neutral head postures ~ Brain mass. The first listed model fails the test suggesting non-normality and the second model passes the test at α <= 0.05.

Test	Model	D	p-value
Lilliefors	Ornstein Uhlenbeck - ln(Neutral head postures) ~ ln(Brain mass).	0.22951	0.001*
Lilliefors	Pagel- ln(Neutral head postures) ~ ln(Brain mass).	0.17267	0.05

When calculating the R-squared, head postures predicted from brain mass under a Pagel correlation structure have a higher R-squared value than the lateral SCC orientation v.s head posture model. The slope and intercept values however are the same as the ordinary least squares model, suggesting that the phylogenetic correlation structure may not be important for the modelling despite the slightly lower AIC score. The p-value is significant (p-value =0.015), and the residuals are approximately normal according to the Lilliefors test (p-value = 0.05).

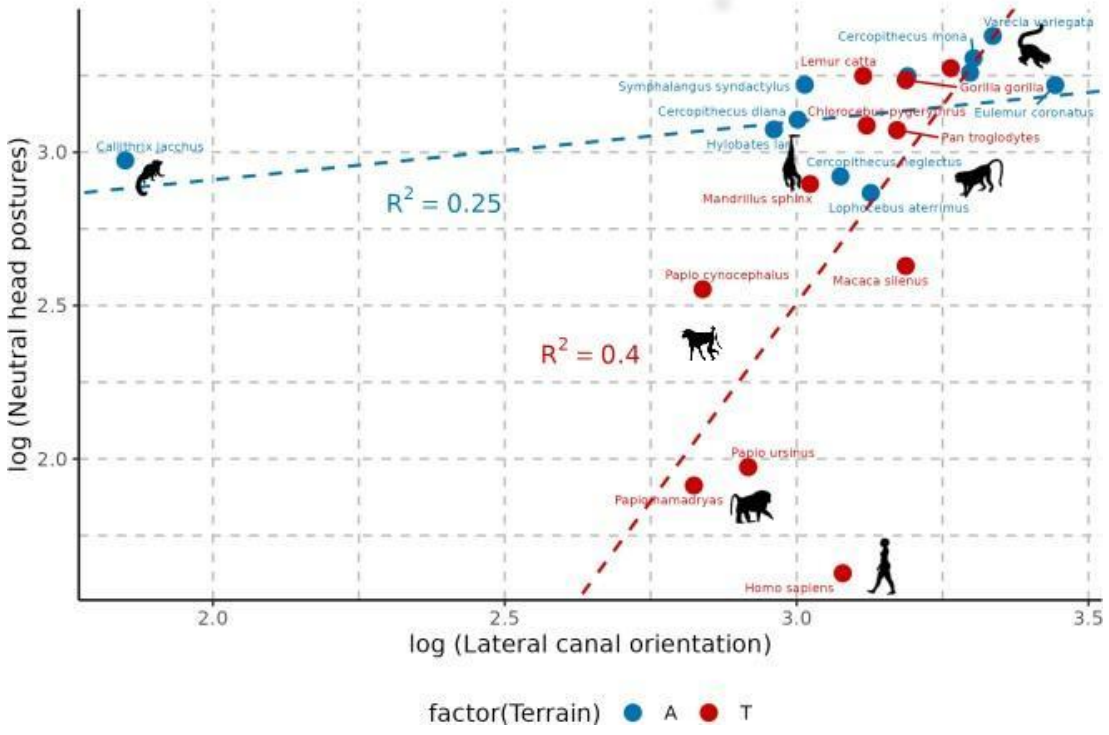

Fig 6.2.1: Neutral head postures ~ Lateral SCC orientation of extant species subsetted according to main substrate (Arboreal and Terrestrial).

Table 6.2.4 – Lilliefors tests for normality for Neutral head postures ~ lateral SCC orientation subsetted by substrate use (Arboreal and Terrestrial). Both results suggest that the regressions are normal.

Model	**Lilliefors test statistic**	**p-value**
Arboreal species	D = 0.23091	0.1037
Terrestrial species	D = 0.20914	0.1963

When regressing at two clade levels, hominoidae and cerocopithecoidea, no significant p-value is recovered for hominoids, with a p =0.1. A significant relationship is, however, recovered for cercopithecoids p = 0.0001. The lillietest results provide support that the data are approximately normal for this clade. A phylogenetic signal of 1 is estimated for hominoids is estimated for the hominoids, but none is present for cercopithecoidea ($\lambda = 0$). This is an interesting result as no signal could be detected in the model using all data points, and may be a consequence of noise produced in the model when the overall tree.

Table 6.2.5: Lilliefors for the PGLS subsetted by two main clades in the sample show no evidence for non normality in the residual structure.

Data	**Lilliefors test statistic**	**p-value**
Cercopithecoids	D= 0.11	p=0.91
Hominoids	D= 0.27	p=0.22

No phylogenetic signal is present ($\lambda = 0$ when subsetting head postures v.s canal orientation according to arboreal and terrestrial substrates. Both models are approximately normally distributed according to the Lilliefors test. This model has a significant p-value for the slope of species coded as terrestrial ($p= 0.03$), but not for arboreal species ($p=0.1$).

6.3 - Fossils

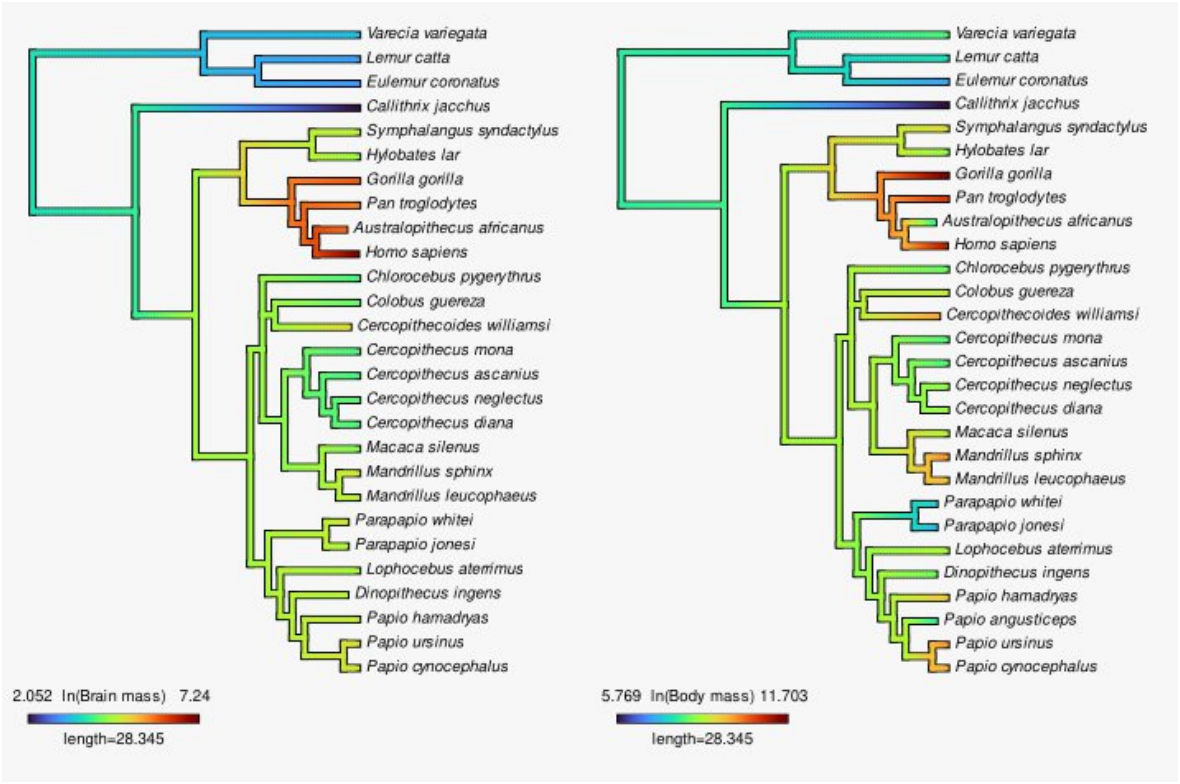

Fig 6.3.1: Phylogenetic trees inferred using total evidence methods in MrBayes used to conduct PCM's, with Ln(Brain mass (g)) and Ln Body mass (g) mapped onto the trees using the 'contmap' function in the 'phytools' package.

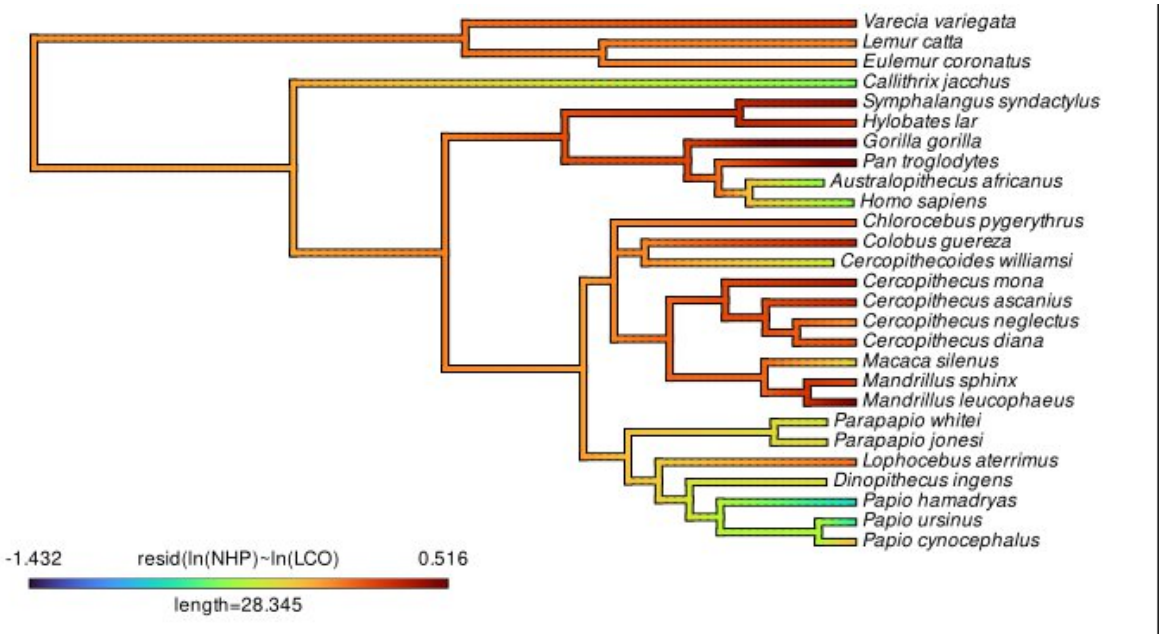

Figure 6.3.2: Ln(NHP) and Ln (LSCC orientation) mapped onto the phylogenetic tree using the ‘contmap’ function from the package ‘phytools’(Revell, 2012). Blues represent lower values, yellow, greem annd orange intermediate and blues lower values.

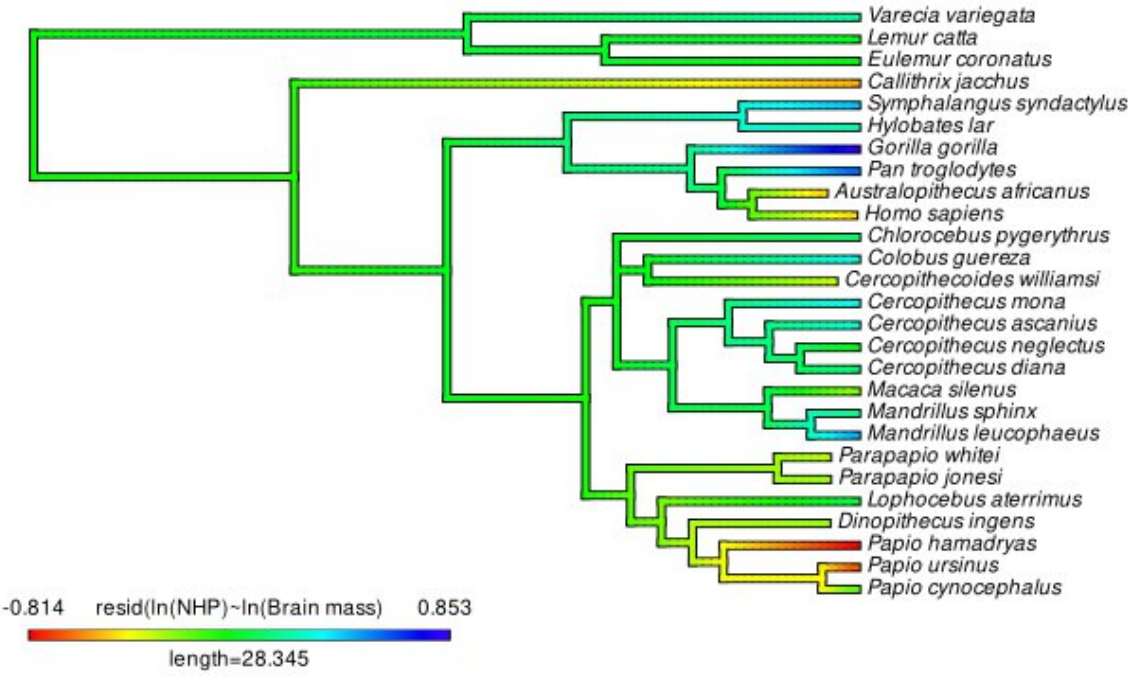

Figure: 6.3.3: Residuals of ln(Neutral head postures) v.s ln(Brain mass) plotted using 'contmap function in phytools (Revell, 2012). Red values are lower values, Red higher, Greens and yellows are intermediate, Blues are higher.

The lateral canal orientations of the fossil cercopithecoids all fall within the mean range of extant Papio species and *Macaca silenus*. *Cercopithecoides williamsi* has an average canal orientation slightly lower than the mean of its closest extant relative in the sample, *Colobus guereza.* One of the *Colobus guereza* specimens, however, has a lower canal orientation than the mean of *C. williamsi (*~ 17.5 3°).

Average values of these two canal orientations for *C. williamsi* cannot therefore be interpreted as a shift toward a different substrate preference or a change in locomotor diversity. Australopithecus africanus (Sts 5), has a mean orientation in the range of arboreal species and knuckle walking apes. Homo sapiens, however, exhibit a mean canal orientation similar to that of baboons (21.73°), but have orientations that range between 14.7° and 30°. Overall, there does appear to be a trend toward arboreal species having a larger angle of the lateral canal relative to the Frankfurt horizontal, with the exception bein*g Callithrix jacchus*, which exhibits the lowest lateral canal angle of all species (6.361°). Included in the discussion. The lower canal angle makes *C. jacchus a* clear outlier among predominantly arboreal species. Given that it is the only platyrrhine sampled, it would be interesting to see if this condition hold across platyrrhini, or it emerged via multiple independent origins, a small face (Bastir et al., 2010), and a low cranial base angle (Ross and Ravosa, 1993), or other cranial attributes.

These results show that while there is substantial variance in canal orientation. average values are similar for primates overall. The full model of head posture predicted from canal orientation with predictions from the terrestrial regression values shows a moderate phylogenetic signal of $\lambda = 0.53$. The model is normal according to the lillietest ($p = 0.1$). When plotting a phylogenetically corrected regression under an Pagel model of neutral head postures v.s lateral SCC orientation for the 2 locomotor modes for which more than 2 species are available, a significant correlation is recovered within for arboreal quadrupeds while terrestrial species fail to meet significance (Table 6.3.1). The model recovers arboreal species as having an R-squared of 0.25, and terrestrial species as having an R-squared of 0.40 and p-values of 0.008 and 0.08 respectively. Results of the lillietest for both terrestrial and arboreal species recover no evidence of non-normality in the residuals. The residual plots however reveal that there is some heteroscedasticity in the models (Table 6.3.1).

Table 6.3.1: p-values for PGLS and Lilliefors tests for normality of best fitting PGLS models. Model fits are improved when subsetting by arboreal and terrestrial substrates with no evidence for non-normality ($p > 0.05$) and the p-value for arboreal species is significant at $\alpha < 0.01$.

Model	**PGLS p-value**	**Lillietest**
Full model Neutral head posture ~ Reconstructed canal orientation (PGLS)	p=0.1	D = 0.19532, p-value = 0.007702
Arboreal species (PGLS)	p=0.008	D = 0.22736, p-value = 0.1155
Terrestrial species (PGLS)	p=0.08	D = 0.12084, p-value = 0.7325

Head postures predicted from canal orientation performs best when subsetting by predominantly terrestrial and predominantly arboreal substrate use. There is no phylogenetic signal present in the residuals from the terrestrial (λ), early burst (EB), and ornstein uhlenbeck (OU) were compared using = 0), or the while the arboreal model as a small amount of phylogenetic signal present (λ), early burst (EB), and ornstein uhlenbeck (OU) were compared using = 0.11). This suggests that the correlation between head posture and canal orientation is a functional one with a moderate amount explained by substrate use.

The phylogenetic signal for canal orientation is high (λ = 0.99), suggesting that the character varies under a Brownian motion model of evolution characterised by a random walk that accrues proportional to the branch lengths along the phylogeny (Münkemüller et al., 2012). The lower proportion of the variance explained by the arboreal model may be due to the single vertical leaper. in the dataset, *Callithrix jacchus,* reducing the steepness of the slope. *Callthrix jacchus* was included since the exclusion of this species resulted in non-normally distributed residuals. Predicting head postures from brain mass across the dataset performs best in that a better overall model fit is achieved which meets model assumptions and meets the threshold for statistical significance.

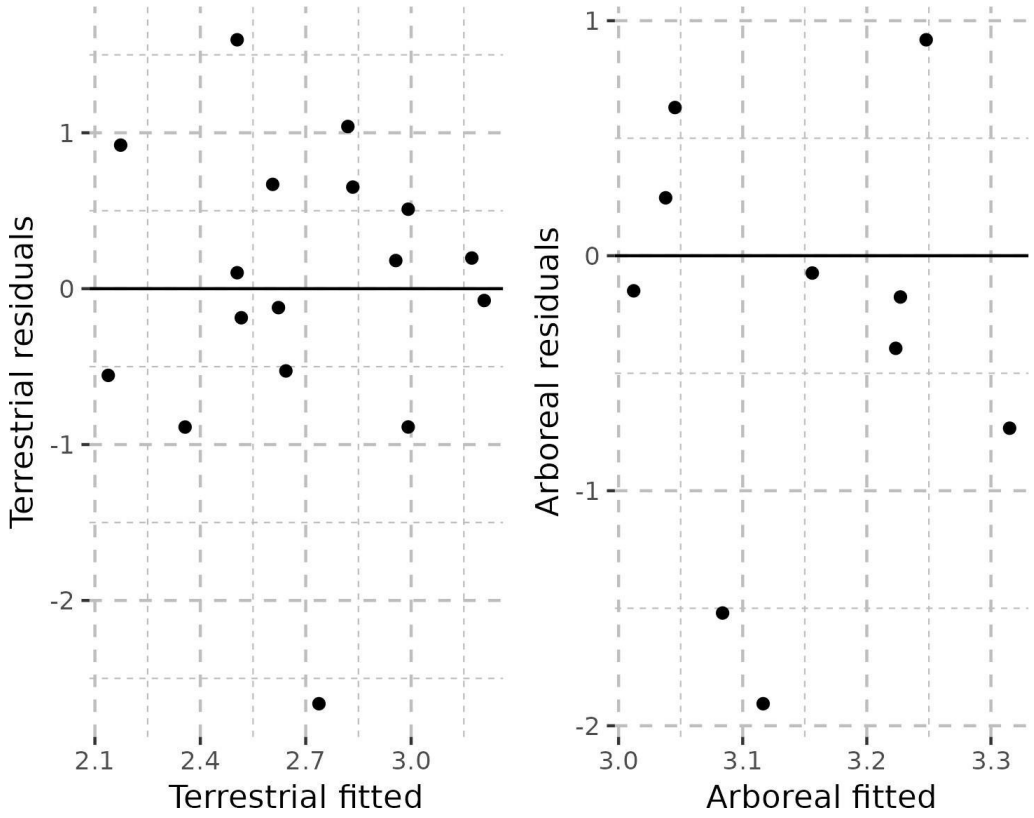

Fig 6.3.4: Residual plot of PGLS of arboreal and terrestrial species. Terrestrial species have one outlier and arboreal species have two. *Homo sapiens is* the largest outlier in the terrestrial dataset followed by Papio species. Since these species are needed to infer the evolutionary pattern of hominins and fossil cercopithecoids they were not dropped from the dataset.

Table 6.3.3: Predicted values from PGLS model under Pagel's lambda of neutral head postures predicted from brain mass. *Australopithecus africanus* and *Cercopithecoides williamsi, Parapapio*

jonesi, *Parapapio whitei*, and *Dinopithecus ingens* exhibit a head posture within the range of the terrestrial condition under the brain mass model.. No brain mass data is available for *Papio angusticeps.* All Parapapio and Papio species are predicted to have similar head postures to modern *Papio cynocephalus*.

Species	**Predicted value for head posture from PGLS (Brain mass)**
Australopithecus africanus	6.82°
Cercopithecoides williamsi	10.38°
Parapapio jonesi	12.42°
Parapapio whitei	11.02°
Dinopithecus ingens	12.30°
Papio angusticeps	-

When using head posture predicted from brain size and phylogenetic ANOVA pairwise comparison, a number of significant values were obtained: knuckle walkers are significantly different to bipeds, bipeds significantly different to arboreal quadrupeds and arboreal quadrupeds are significantly different to terrestrial quadrupeds (Table 6.3.4). No significant difference is recovered between brachiators and any other modes and bipeds do not exhibit significantly different brain size from terrestrial quadrupeds (Table 6.3.4). This is probably due to *A. africanus* displaying a brain size closer to the great ape condition, and/or the head postures of baboons recovered in an outlying position along with *H. sapiens.*

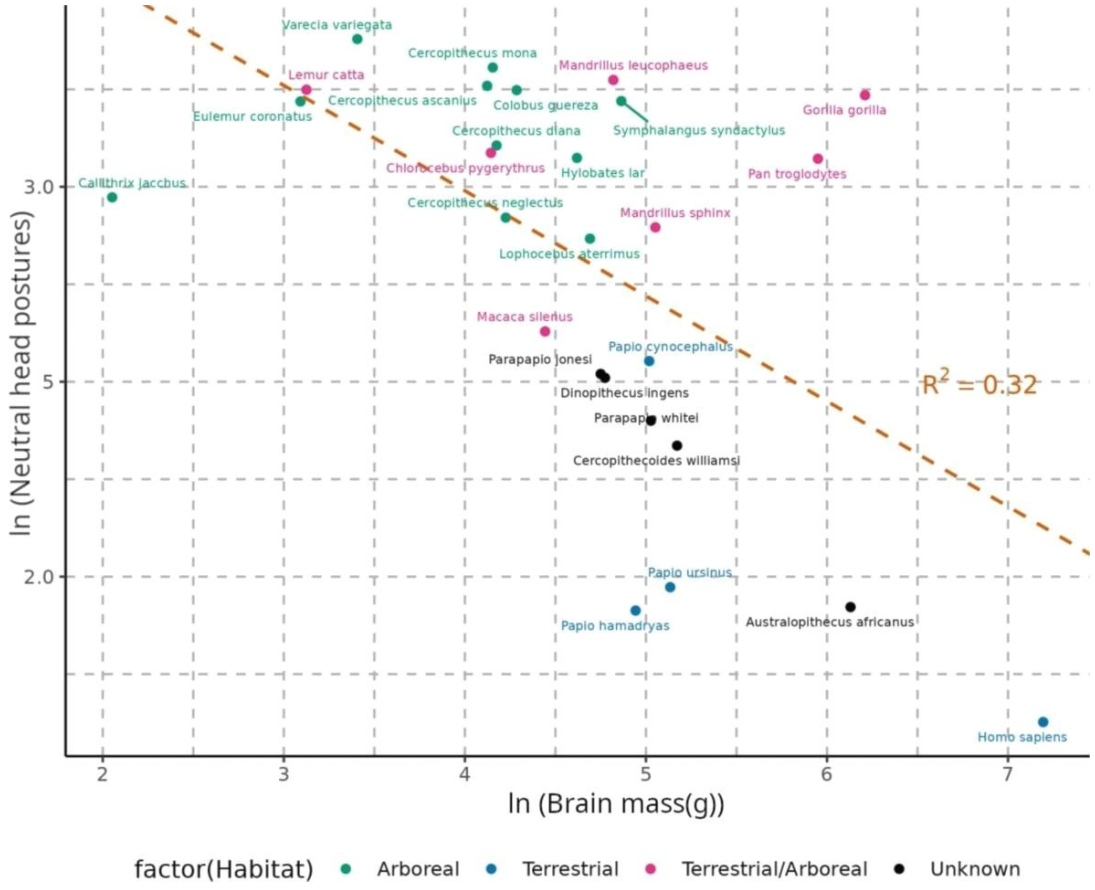

Fig 6.3.5: Results of PGLS of head postures v.s brain mass. Here fossils are treated as unknown. All fossil species can be seen plotting closer to terrestrial ones. In contrast to the predictions from the regression subsetted by substrate use (habitat), this model recovers *A. africanus* as having a similar posture to *H. sapiens.* Fossil cercopithecoids all plot in the region of extant baboons (terrestrial) and *Macaca silenus* (semi-terrestrial).

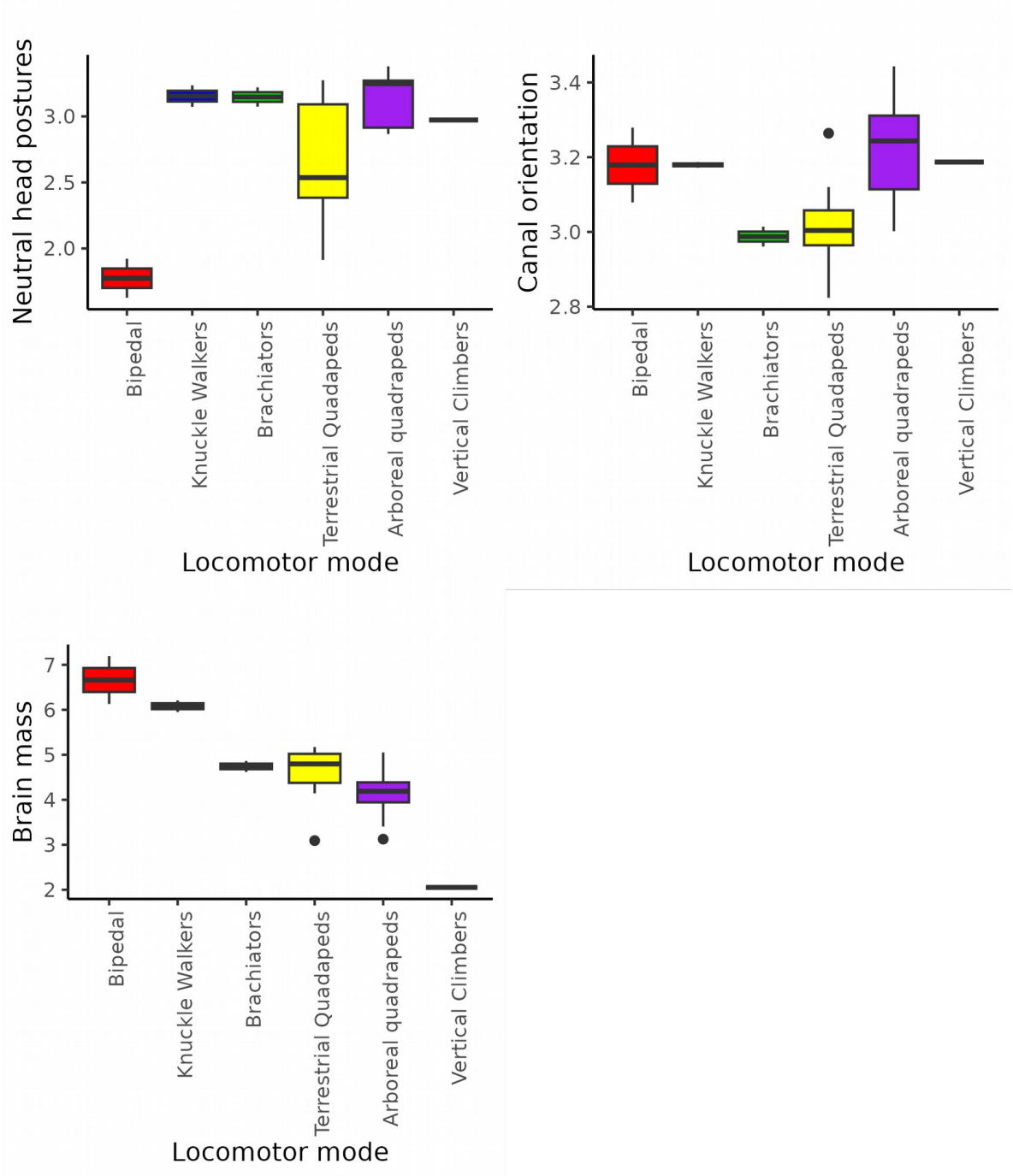

Fig 6.3.6: Locomotor box-plots of main locomotor modes and selection of variables examined under phylogenetic regressions in this study. Predicted values for fossils included in these plots are estimated from PGLS prediction done on brain mass.

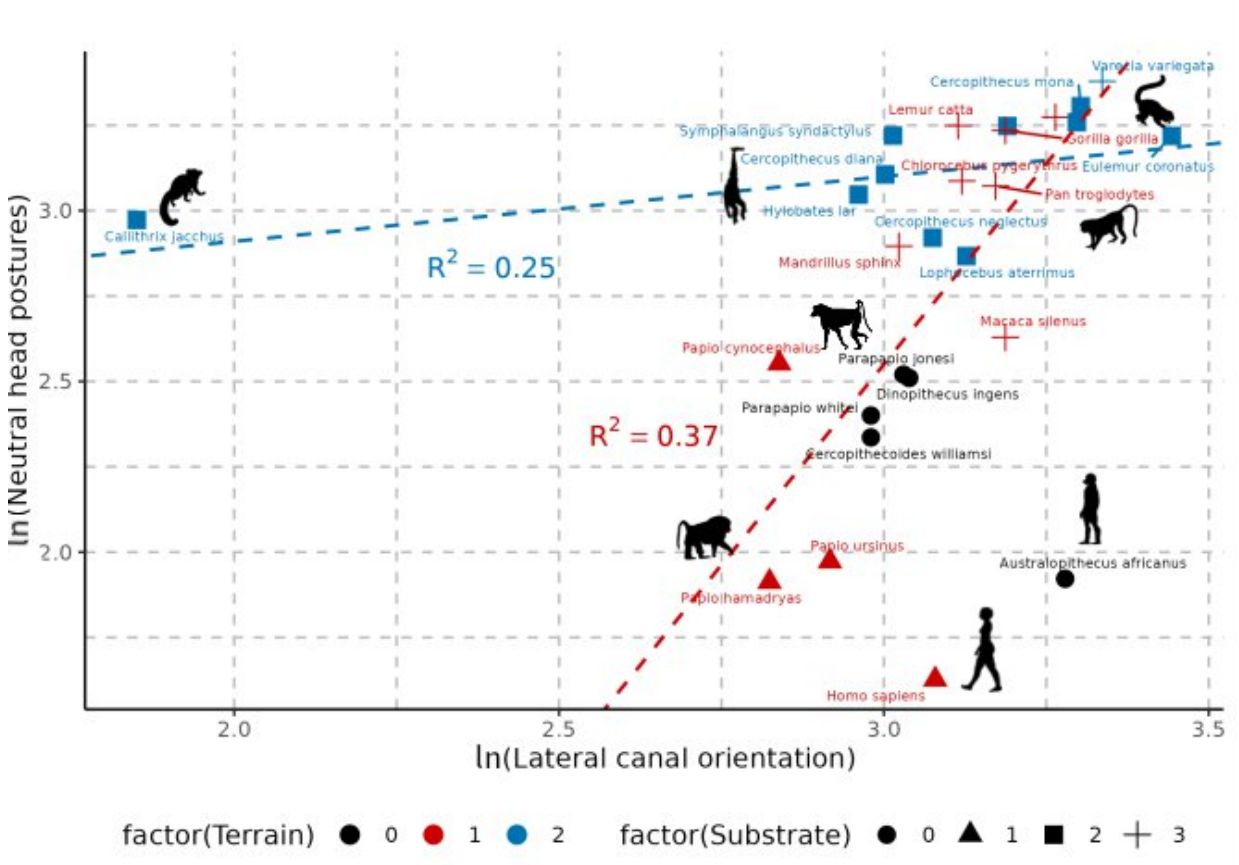

Fig 6.3.7: PGLS sub-setted by arboreal (blue) and terrestrial species (red). Fossils (black circles) head posture values are predicted from brain mass. Crosses (substrate factor 3) are semi-terrestrial species.

Table 6.3.4: Kruskal-Wallis paired comparisons of residuals from Neutral head postures v.s canal

orientation: No significant difference is recovered between groups.

Bipedalism	**Knuckle walker**	**Brachiator**	**Arboreal quadruped**	**Terrestrial quadruped**
p=1	p=0.08	0.648	p=1	p=1
p=0.08	p=1	p=1	p=1	p=1
p=0.648	p=1	p=1	p=1	p=1
p=1	p=1	p=1	p=1	p=0.648
p=1	p=1	p=1	p=0.648	p=1

Table 6.3.5 Pairwise corrected p-values from phylogenetic anova with predicted values for fossils for neutral head posture from brain mass. Significant values are recovered between all groups except for brachiators and all other groups and bipeds and other terrestrial quadrupeds. The lack of difference between bipeds and terrestrial quadrupeds is likely due to baboons sometimes adopting similar postures. * = significant at α= 0.05.

	Bipedalism	**Knuckle walker**	**Brachiator**	**Arboreal quadruped**	**Terrestrial quadruped**
Bipedalism	p=1.000	p=0.010*	p=0.112	p=0.570*	p=0.119
Knuckle walker	p=0.010*	p=1.000	p=1.000	p=1.000	p=1.000
Brachiator	p=0.112	p=1.000	p=1.000	p=1.000	p=1.000
Arboreal quadruped	p=0.570*	p=1.000	p=1.000	p=1.000	p=0.045*
Terrestrial	p=0.119	p=1.000	p=1.000	p=0.045*	p= 1.000

quadruped					

Table 6.3.6: Phylogenetic anova pairwise comparisons between species coded as arboreal and terrestrial. All 3 variables: canal orientation, head posture and brain size are significantly different. Fossil predictions in this model are from brain mass.

Model	Comparison: Arboreal/Terrestrial
Lateral canal orientation ~ Terrain	p=0.011**
Neutral head posture ~ Terrain	p=0.005**
Brain mass ~ Terrain	p=0.04*

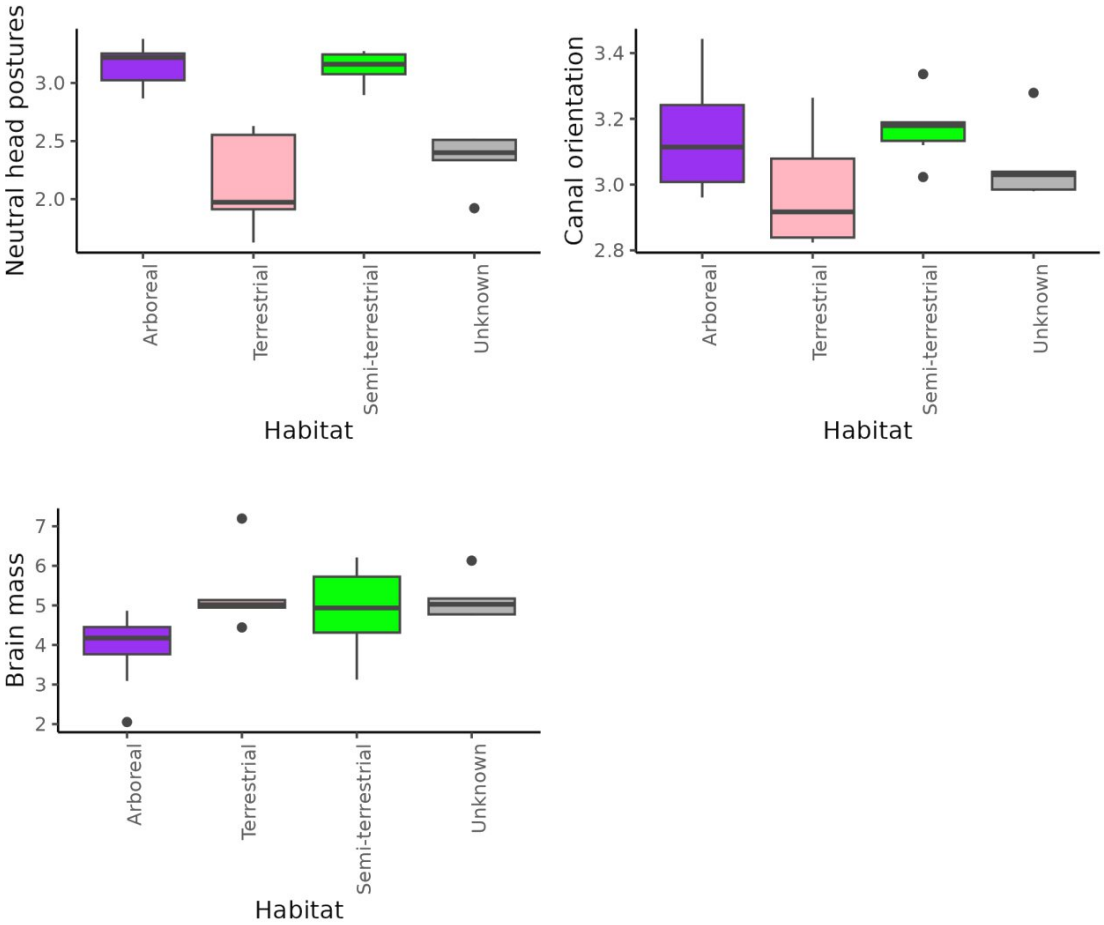

Fig 6.3.8: Box-plots of habitat (substrate use) v.s head postures, canal orientation and brain mass. Under this model are fossils treated as 'unknown" in grey and values are predicted from brain mass.

Table 6.3.7: pairwise phyloanova p-values of neutral head postures subsetted by substrate with coding 'semi- terrestrial' included. Fossils are coded as unknown. No significant differences are recovered.

	Arboreal	**Terrestrial**	**Semi-terrestrial**	**Unknown**
Arboreal	p=1.000	p=0.390	p=0.940	p=0.635
Terrestrial	p=0.390	p=1.000	p=1.000	p=1.000
Semi-terrestrial	p=0.940	p=1.000	p=1.000	p=1.000
Unknown	p=0.635	p=1.000	p=1.000	p=1.000

Table 6.3.8: pairwise phylo anova p-values of lateral SCC orientation by substrate use. No significant differences are recovered.

	Arboreal	**Terrestrial**	**Semi-terrestrial**	**Unknown**
Arboreal	p=1.000	p=0.23	p=0.816	p=0.816
Terrestrial	p=0.230	p=1.000	p= 0.120	p=0.380
Semi-terrestrial	p=0.816	p=0.12	p= 0.468	p=0.468
Unknown	p=0.816	p=0.38	p=1.000	p=1.000

Table 6.3.9: Phylogenetic regressions of substrate use (terrestrial, semi-terrestrial, arboreal, unknown) against neutral head posture (predictions for fossils from from brain mass). The model is recovers a significant intercept at significant $\alpha < 0.001$ ***.

Model	Intercept p-value	Slope p -value	R^2
Substrate use v.s Neutral head postures	p=0.0165495 *	p=0.0001895 ***	0.40

CHAPTER 7 – DISCUSSION

7.1 - Neutral head posture v.s lateral canal orientation

This project's main objective was to examine the relationship between the lateral SCC and neutral head postures in primates, and test whether it is aligned with earth's horizontal at rest. The lateral SCC canals have been argued to be aligned to the yaw plane of head which is maximally sensitive when parallel with earth's horizontal plane (Girard, 1923; Muller and Verhagen, 2002; Fitzpatrick et al., 2006; Hullar, 2006; David et al., 2010). However, despite suggestions that the lateral SCC's are held close to the horizontal at rest across taxa (Girard, 1910, 1923, 1924, 1929; Perez, 1922; de Beer, 1947; Delattre and Anthony, 1951; Delattre and Fenart, 1957, 1958; Vidal et al., 1986; Spoor and Zonneveld, 1998c; Fitzpatrick et al., 2006; Hullar, 2006; Coutier et al., 2017; Schellhorn, 2018; Le Maître, 2019), the results here show that this is not consistently the case. The high phylogenetic signal (λ= 0.99) recovered for Lateral SSC orientation reveals that the character is highly heritable and under the constraints of phylogeny. Lateral SSC orientation varies little between species and therefore most of the variance is exhibited in head posture (Appendix Table 3). The results of phylogenetic signal on head posture alone is λ =0. It is therefore unlikely that neutral head posture and canal orientation are evolving in a correlated fashion. These results are therefore in broad agreement with Benoit et al. (2020), where it is suggested caution should be exercised when trying to infer head posture in fossil species on the basis of the lateral canal. Furthermore, the Kruskal Wallis comparisons of residuals from PGLS of Neutral head postures ~ Lateral SCC orientation corroborate that canal orientation alone is not useful for predicting locomotion in primates (Table 6.3.8).

Canal orientation approximately aligns with earth's horizontal in *Cercopithecus diana, Cercopithecus mona, Cercopithecus ascanius, Hylobates lar, Symphalangus syndactylus, Gorilla gorilla, Pan troglodytes, Mandrillus leucophaeus, Mandrillus sphinx, Varecia variegata, Lemur catta*, and *Eulemur corantus* (Appendix Table 3, Fig 6.2.1, Fig 6.3.7). However, the lack of consistency across primates suggests that bringing the lateral canal near the horizontal is not functionally important as has been historically argued (Girard, 1910, 1923, 1924, 1929; Perez, 1922; de Beer, 1947; Delattre and Anthony, 1951; Delattre and Fenart, 1957, 1958; Vidal et al., 1986; Spoor and Zonneveld, 1998; Fitzpatrick et al., 2006; Hullar, 2006; Coutier et al., 2017; Schellhorn, 2018; Le Maître, 2019). The residual mapping of Ln(Neutral head postures v.s Ln(Lateral canal orientation) in Figure 6.3.3, show that lower values tend to be highly terrestrial species (e.g. papio species, Homo) and higher values tend to be arboreal (e.g. C*ercopithcecus mona, Cercopithecus ascanius, Varecia variegata*) , a glaring exception being *Callthrix jacchus.*

When the canal is held horizontal, the head is characterised by a slight pitch forward (Figure 2.1). Arboreal species appear to adopt less orthograde postures when resting (Appendix Table 2, Appendix Table 3). The postural hypothesis that suggests that a more pronograde neck would need to be more flexible to orient the orbits anteriorly and a more orthograde neck would require a more flexed base to attain anterior orbital orientation (Strait and Ross, 1999), may explain this pattern. A head posture characterised by a slight pitch forward may improve reaction during vigilance behaviours by permitting quicker refuge and concealment from predators in arboreal species. This conjecture may be tested using a combination of photographic and non-invasive eye tracking techniques (see Howard and Lonsdorf, 2022), followed by assessing these against anatomical characteristics related to head posture. The levels of asymmetry among some specimens detected in this study (Appendix: Table 1)

are higher than what has been reported in other primates (Lebrun et al., 2021). In future studies it would be important to analyse potential functional reasons for this asymmetry.

7.2- Obligate terrestriality

It is striking that the lateral canal is significantly different between two substrates (‘arboreal and terrestrial’) as is neutral head posture (Table 6.3.6). The plots (Fig 6.2.1, Fig 6.3.7) clearly display *Papio, Parapapio,* and *Homo* as outliers to the arboreal regression line, fitting on a completely different, much steeper line (Fig 6.3.7). *Parapapio, Papio, and hominins* are widely considered to have transitioned from wooded environments to grassland during the late-pliocene early pleistocene (e.g. Vrba, 1985; Potts, 1998a, 1998b; Bobe and Behrensmeyer, 2004). That terrestrial and arboreal species differ in head posture may can be accounted for by the coupling of the LSC with other aspects of the basicranium (Spoor and Zonneveld, 1998) and with differing visual demands encountered in an arboreal v.s terrestrial environment.

Lateral SCC orientation has already been suggested to correlate with orbital orientation (Lieberman et al., 2000). Therefore the changes detected between head posture lateral SSC orientation may in part be accounted for by the challenges of a 3 dimensional environment where arboreal species need to stabilise themselves on narrow supports v.s a 2 dimensional environment in terrestrial species (Preuschoft and Franzen, 2012). The overlap of semi-terrestrial forest dwelling taxa (Fig 6.2.1, Fig 6.3.7), suggests that these may have retained an arboreal attitude of the head in relation to the lateral canal.

Among terrestrial species, *Homo* is an outlier (Figs. 6.2.1, Fig 6.3.5, Fig 6.3.7). The extreme outlying position of *H. sapiens*, corroborates previous observations whereby *H. sapiens* are notably deviant in the angle between head posture and lateral canal orientation (e.g. de Beer, 1947). The outlying position of *H. sapiens* among terrestrial species hominoids may be explained by the increase in encephalization in *H. sapiens*, whereby an expanding brain changes the orientation of the brain case and in turn the lateral SCC or the reduction in size of the lateral SCC due to relaxed selection on yaw movements being rare in *H. sapiens* (Lieberman, 2011). The convergence of outlying status in *Homo* and *Papio* species is likely driven by an increasingly terrestrial habit in these clades. The results show that hominoids exhibit a phylogenetic signal of lambda(λ) = 1, which suggests that these traits are correlated under a neutral, Brownian motion model of evolution (Revell et al., 2008). Cercopithecoids, by contrast, exhibit no phylogenetic signal, suggesting that posture in this clade was under functional selection for an increasingly terrestrial lifestyle.

The results of the outlying position of baboons and humans are broadly consistent with other research that found convergence in angles of the SCC and aspects of the basicranium Spoor and Zonneveld (1998). *Papio* and *H. sapiens* also tend to hold their heads pitched slightly upward or straightforward (Appendix Table 2, Appendix Table 3, Figure 7.2.1). The results of the study show, that overall, terrestriality is reflected in the relationship between neutral postures and lateral canal orientation. This has important implications for reconstructing ecological preferences and arborealism and terrestrialism in extinct species and bipedalism in hominins. This holds important implications on reconstructing terrestriality in extinct hominins.

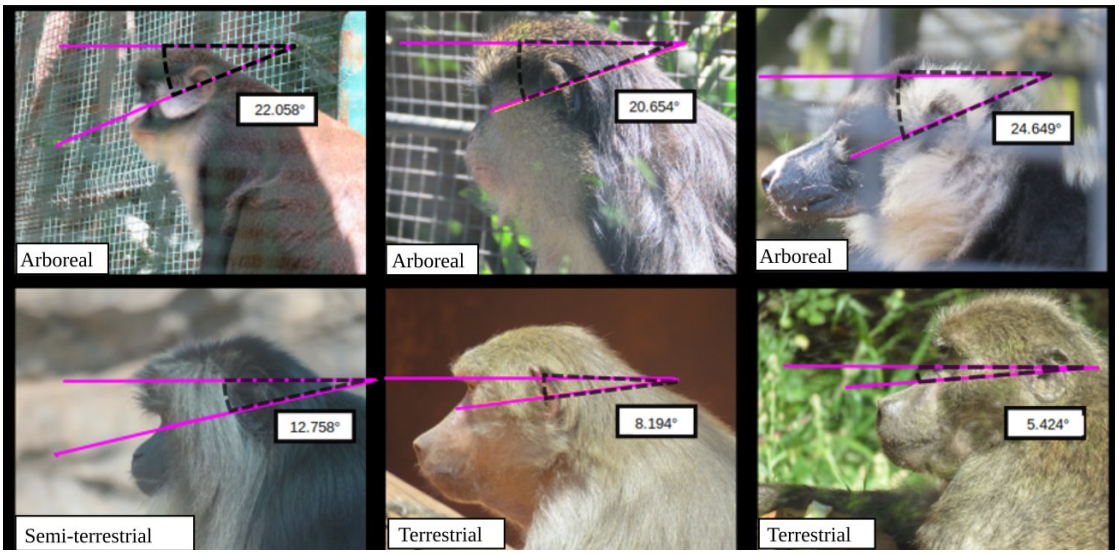

Fig 7.2.1 : Photos of arboreal species in the top row from left to right (*Cercopithecus ascanius, Cercopithecus mona*, *Varecia Variegata.* Predominantly terrestrial species in bottom row from left to right (*Macaca silenus, Papio hamadryas* and *Papio ursinus)*. Note the larger angle between the Frankfurt horizontal in the arboreal species v.s smaller angle in predominantly terrestrial species.

7.3 - Can Bipedalism be inferred from Lateral SSC orientation?

Lateral SCC canal orientation is expected to correlate with locomotion due to the demands placed on the vestibular system during movement, and when an animal needs to stabilise gaze and head posture (Sanders and Smith, 2005; Bullar et al., 2019), and bipedalism is expected to be associated with changes in the semicircular canals given the demands of maintaining an upright posture over a small area of support (Spoor et al., 1994).

This study sought to address if lateral SCC orientation was correlated with locomotion using photographs taken with a spirit level, digital segmentation techniques, and statistical methods. The

results suggest that lateral SCC orientation is not the most important variable for inferring locomotor behaviours (Fig 6.1.2, Fig 6.3.6, Table 6.1.2, Table 6.3.6). Indeed, neutral head posture alone is a better overall predictor of main locomotor modes (terrestrial quadrupedalism, arboreal quadrupedalism and knuckle walking) (Fig 6.3.6, Table 6.3.5), with no significant difference found between brachiation and other locomotor modes (Table 6.3.5). The functional importance of the orientation of the canal during locomotor behaviours may be better explained, like other aspects of SCC morphology, by cranial integration as has been found in other amniote clades (Bronzati et al., 2021b; Evers et al., 2022). Alternatively, the plane of sensitivity may be maximised and under selection when the animal is moving or during yaw movements (Spoor and Zonneveld, 1998). During movement an animal may pitch its head forward, bringing its canals in line with earth's horizontal (Urciuoli et al., 2020). Indeed, physiological data has shown that in humans the lateral SCC only senses 62% of the angular acceleration vector at rest in contrast to 99% when pitched forward (Fetter et al., 1986).

Overall, lateral canal orientation is not a good predictor of primary locomotor mode or positional repertoires (as denoted by the locomotor diversity index). Neutral head posture may, however, be predicted if information about substrate preferences is available (arboreal v.s terrestrial). However, this study did not assume a priori that the species under consideration had a known substrate preference. Hence, lateral canal orientation was not used to make predictions. Importantly, despite documentation about the importance of the lateral semicircular canals in stabilising posture (e.g. Fitzpatrick et al., 2006; Day et al., 2010), lateral canal orientation does not provide information about bipedalism in hominins. It would be interesting to see if these methods can be investigated in archosaurs where the lateral canal is so often claimed to be a reliable proxy for head posture (e.g. Sanders and Smith, 2005; Bullar et al., 2019).

7.4- Brain mass

Surprisingly, brain mass is found to be a good predictor of neutral head posture (Fig 6.1.1, Fig 6.1.2, Fig 6.3.6). Additionally, the results of the regression of neutral head postures v.s brain mass, using brain mass as a predictor of for fossil values f(Fig 6.3.3), supports brain mass as explaining a significant proportion of the variance ($R^2 = 0.32$, $p=0.0001$). Smaller brained primates generally adopt a posture where their heads are more tilted (Fig 7.2.1, Appendix Table 2). The relationship is not entirely straightforward, however, as chimpanzees have more ventrally tilted neutral head postures than baboons (Appendix Table 2, Appendix Figure 1). This is also displayed in the character mapping of neutral head postures v.s lateral SCC orientation (Figure 6.3.3). Differences in brain shape and proportions may account for these differences. Changes in brain shape are characterised by lateral and posterior expansion in Papionins, and an anterior expansion in hominoids (Sansalone et al., 2020).

Allometrically driven evolutionary accelerations in brain shape in hominoids and papionins have been suggested to account for complex behaviours which, in turn, are reflected in ecological and positional behaviours (Sansalone et al., 2020). It would be interesting to explore these changes in relation to locomotion and posture in the future.

Aspects of brain development have long been associated with bony labyrinth morphology (Werner, 1933; Spoor and Zonneveld, 1998).The results of the present study are consistent with these studies and provide support to relationships recovered between labyrinthine morphology and brain size (Morimoto et al., 2020). These results may be explained by the spatial packing hypothesis (Bieger1957; Gould, 1977; Moss, 1958; Ross and Ravosa, 1993; Spoor, 1997; Lesciotto and

Richtsmeier, 2019). This hypothesis proposes encephalization plays on basicranial architecture and orientation (Gould, 1975; Spoor and Zonneveld, 1998; Jeffery and Spoor, 2006; Lebrun et al., 2012; Malinzak et al., 2012b; Bastir and Rosas, 2016; Neaux et al., 2019). It has been noted that if labyrinthine angles are expected to be correlated with the rotation of the tentorium cerebelli during ontogeny, relative brain size may correlate with labyrinthine orientation (Spoor and Zonneveld, 1998; Spoor, 2003). In addition to brain size, facial orientation has been demonstrated to explain a proportion of variance in basicranial morphology (Bastir et al., 2010). The position of *Homo sapiens*, in particular, may be a consequence of flexion along the midline of the basicranium (Strait and Ross, 1999; Lieberman et al., 2002; Bastir et al., 2010).

Overall, the results of this study show that brain mass is a good predictor of neutral head posture in fossil species, and shows significant differences between primary locomotor modes. Given that brain mass has been studied extensively in hominins (e.g. Wolpoff, 1981; Jeffery and Spoor, 2002; Deaner et al., 2007; de Sousa and Cunha, 2012; Schoenemann, 2013; Zollikofer and De León, 2013; Grabowski, 2016; Du et al., 2018; González-Forero and Gardner, 2018; Montgomery, 2018; Beaudet et al., 2019, 2021; Cofran, 2019), and primates (eg Sawaguchi, 1990; Ross and Henneberg, 1995; Deaner et al., 2007; Isler et al., 2008; Van Woerden et al., 2010; Herculano-Houzel and Kaas, 2011; Montgomery, 2013; Beaudet et al., 2016; Halley and Deacon, 2017; Powell et al., 2017; Beaudet and Gilissen, 2018; Ni et al., 2019) , the suggested relationship between brain mass and head posture opens up new opportunities for research into this area.

7.5 - Implications for fossil data and the evolution of hominin terrestralisation

As discussed in the previous sections, neutral head postures can be predicted from brain mass in fossil species and Lateral SSC orientation can be extracted directly from fossils. The combination of these data can be used to corroborate whether or not a selected sample of fossils were predominantly terrestrial or arboreal. The results of this study suggests that *A. africanus (Sts 5)* was a predominantly terrestrial species (Fig 6.3.7). These results are consistent with studies which suggest that Australopithecus species were committed terrestrial bipeds (e.g. Green et al., 2007; Ward et al., 2011; Ryan et al., 2018).

Additionally, the results for the fossil cercopithecoids analysed in this study (*P. Jonesi, P. whitei, C. williamsi,* and *D. ingens*) are consistent with a body of research that has argued that these species are all highly terrestrial (e.g. Codron et al., 2005; Gommery et al., 2014; Williams and Geissler, 2014). These results are also not surprising given the relationship that body mass has in hindering arboreal activities (e.g. Delson et al., 2000). Overall, the technique of using brain mass to reconstruct head posture and then projecting these points back into regression space of neutral head postures v.s lateral canal orientation, offers a promising method for inferring whether an extinct species was arboreal or terrestrial.

7.6 - Potential drawbacks

This study did not account for intraspecific or interspecific variation, nor was sexual dimorphism included as a potentially confounding aspect upon neutral head postures, LSCC orienation or brain mass. Primate that have high levels of dimorphism in this study include hominoidae (Schaefer et al., 2004; Higgins et al., 2004), and papionini (Singleton et al., 2012; Singleton et al., 2017). Intra and Interspecific variability can be investigated between brain mass and canal orientation in future studies. However associations between canal orientations in ct-scans and photographs in the same specimens is not feasible without sacrificing the animal. Thus, this study sought to do extensive sampling to achieve statistical power to attain substantial accuracy in a non-invasive manner.

CONCLUSION

Contrary to expectations that bipedalism can be reconstructed on the basis of the plane of the lateral canal in relation to head posture, this study reveals that this is not the case. However, brain mass and head posture are correlated and correlations between neutral head postures and lateral SCC orientation are detected when considered arboreality and terrestriality. A new method is introduced when reconstructing the evolution of terrestriality using brain mass to predict head posture and then comparing these to Lateral SCC orientation, when subsetted by substrate type. The results are consistent with research that suggests that *Parapapio*, *C. williamsi,* and *A. africanus* were all highly terrestrial. These results open up future prospects for studying locomotion using aspects of the cranium, including the brain and the bony labyrinth.

APPENDIX

Table 1: Specimens used in this study to extract lateral canal orientation. L= left R = Right lateral canal orientation in degrees. Abbreviations: PRICT – Kyoto university digital museum; MCZ - Museum of comparative zoology, Harvard university; AMNH – American Museum of Natural history; ESRF- European synchrotron research facility; Isem - Institut des Sciences de l'Evolution de Montpellier; sbu – Stony Brook University. SIU – Southern Illinois University; DLC – Duke University Lemur Centre; PBC – Pretoria bone collection – University of Pretoria; Dnmnh- Ditsong natural history museum.

Taxon	**Specimen**	**L**	**R**
Homo sapiens	PBC 2615	22.8°	29.3°
Homo sapiens	PBC 2452	30.5°	14.7°
Homo sapiens	PBC 3866	18.2°	21.4°
Homo sapiens	PBC 3669	18.9°	22.3°
Homo sapiens	PBC 4253	15.3°	20.3°
Australopithecus africanus	Wits- Sts 5	25.7°	27.4°
Pan troglodytes	PRICT 22	24°	19.7°
Pan troglodytes	MCZ: mamm 15312	21.6°	19.2°
Pan troglodytes	MCZ:mamm:bom-6244	21.5°	21.3°
Pan troglodytes	Isem: AG 06	20.9°	31.2°
Pan troglodytes	PRICT 147	22.7°	36.35°
Gorilla gorilla	PRICT 1345	20.64°	20.313°
Gorilla gorilla	MCZ:mamm:26850	22.3°	19.5°
Gorilla gorilla	PRICT 145	22.22°	17.9°
Gorilla gorilla	ESRF 50001988	27.4°	30.4°
Gorilla gorilla	PRICT 2774	26.5°	31.4°
Hylobates lar	PRICT 1287	19.96°	19.449°

Hylobates lar	ESRF 500114	19.3°	22.1°
Symphalangus syndactyalus	PRICT 1083	26.3°	22.3°
Symphalangus syndactyalus	MCZ:mamm:36031	20.3°	26.6°
Symphalangus synadactyalus	MCZ:mamm:36032	21.3°	18.8°
Papio angusticeps	Dnmnh-KA 194	-	19.8°
Dinopithecus ingens	Dnmnh- SK 554	20.1°	21.7°
Parapapio jonesi	Dnmnh- Sts 565	24.7°	16.7°
Parapapio whitei	Dnmnh-MP-221	18.4°	-
Papio ursinus	sbu: RS PU-B	21.1°	14.9°
Papio ursinus	sbu: RS PU-F	9.3°	15.3°
Papio ursinus	sbu: RS PU-C	26°	23.9°
Papio ursinus	sbu: RS PU-E	16.74°	15.32°
Papio cynocephalus	AMNH 54227	17.5°	16.7°
Papio hamadyras	PRICT 93	13.81°	13.008°
Papio hamadyras	PRICT 256	21.1°	19.3°
Papio hamadryas	PRICT 424	16.98°	NA
Lophocebus aterrimus	AMNH 82428	32.22°	27.81°
Lophocebus aterrimus	AMNH 86705	17.3°	13.9°
Lophocebus aterrimus	AMNH 55013	20.6°	20.5°
Mandrillus sphinx	AMNH:anth:99.1-2056	24.5°	27.8°
Mandrillus sphinx	AMNH:anth:99.1-1296	27.1°	15.6°
Mandrillus leucophaeus	MCZ:mamm:19986	21.5°	31.5°
Mandrillus leucophaeus	MCZ:mamm:23169	32.4°	28.8°
Mandrillus leucophaeus	MCZ:mamm:23168	26.8°	17.6°
Macaca silenus	PRICT 1150	25.04°	31.2°
Macaca silenus	PRICT 1148	25°	28°
Macaca silenus	PRICT 424	20.2°	20.2°
Macaca silenus	PRICT 1121	29.2°	15.2°

Cercopithecus neglectus	PRICT 254	24.6°	17.75°
Cercopithecus neglectus	sbu:RS 85 3	17.74°	24.56°
Cercopithecus neglectus	sbu:RS 81 9	28.8°	27.6°
Cercopithecus mona	OCR6	36.4°	28.7°
Cercopithecus mona	sbu: RS 93 1	-	29.69°
Cercopithecus ascanius	sbu: RS8 5	29.2°	21.1°
Cercopithecus ascanius	sbu: RS8 6	26.56°	31.29°
Cercopithecus ascanius	sbu: RS8 13	29.9°	30.8°
Cercopithecus diana	sbu:YPM 006020	26°	27.7°
Cercopithecus diana	PRICT 1509	25.3°	21.6°
Cercopithecus mona	PRICT 969	21.7°	22°
Chlorocebus pygerythrus	SIU 5591	21.26°	24.1°
Chlorocebus pygerythrus	SIU 4817	21.1°	24.1°
Chlorocebus pygerythrus	SIU 4815	25°	21.8°
Colobus guereza	PRICT 938	23.43°	24.12°
Colobus guereza	PRICT 55	32.8°	30.26°
Colobus guereza	AMNH 52249	17.4°	17.7°
Cercopithecoides Williamsi	Wits- MP 3a	19.2°	20.2°
Lemur catta	DLC 7142	20.196°	20.204°
Lemur catta	MCZ 44903	23.8°	27.3°
Lemur catta	DLC6267f	24.1°	25.7°
Eulemur coranatus	DLC 5937	38°	30.8°
Eulemur coranatus	DLC 6034	32°	35.2°
Eulemur coranatus	DLC 6177F	31.2°	31.7°
Eulemur coranatus	DLC 6035	28.5°	22.9°
Varecia variegata	AMNH 201395	27.2°	23.8°
Varecia variegata	AMNH 10050	33°	27.4°

Varecia variegata	AMNH 100511	32°	25.4°
Callithrix jacchus	MCZ:mamm:37823	6.3°	5.1°
Callithrix jacchus	USNM:mammals:503885	6.47°	6.9°
Callithrix jacchus	AMNH:Mammals:M-200525	5°	8.4°

Table 2: Measurements of photographs of neutral head postures. A1, A2 and A3 refer to the the same measurement done 3 times to correct for intra-observer error. Measurements above 3 standard deviations are flagged below and were excluded from the analysis. This was done since inter and intraspecific variation could not be compared across the photographs and ct-scans due to these different individuals analysed in each data-set.

Taxon	Measurement 1	Measurement 2	Measurement 3
Homo sapiens	10.773°	12.366°	11.104°
Homo sapiens	8.497°	8.873°	11.008°
Homo sapiens	10.072°	10.429°	11.872°
Homo sapiens	9.866°	4.664°	8.537°
Homo sapiens	7.727°	5.693°	4.249°
Homo sapiens	6.041°	5.641°	6.056°
Homo sapiens	1.936°	5.332°	5.999°
Homo sapiens	2.991°	6.85°	4.804°
Homo sapiens	12.02°	10.999°	11.705°
Homo sapiens	12.433°	12.095°	13.57°
Homo sapiens	6.305°	6.287°	1.336°
Homo sapiens	1.009°	1.838°	1.7°
Homo sapiens	1.575°	0.202°	1.432°
Homo sapiens	1.874°	3.066°	0.642°
Homo sapiens	3.77°	0.813°	10.412°
Homo sapiens	0°	4.942°	5.359°
Homo sapiens	2.717°	4.751°	6.25°
Homo sapiens	5.227°	8.13°	6.039°
Homo sapiens	3.769°	6.116°	3.343°
Homo sapiens	3.145°	1.718°	2.556°
Homo sapiens	3.19°	1.718°	2.558°
Homo sapiens	4.618°	0.429°	2.81°
Homo sapiens	0.29°	7.716°	2.298°
Homo sapiens	2.397°	2.252°	4.255°
Homo sapiens	3.691°	2.006°	5.823°
Homo sapiens	3.537°	4.163°	4.32°
Homo sapiens	0.739°	1.666°	1.38°
Homo sapiens	1.87°	2°	2.396°
Homo sapiens	4.055°	0.789°	1.41°
Homo sapiens	3.357°	1.172°	0.185°
Homo sapiens	5.563°	1.73°	2.842°
Homo sapiens	3.945°	1.522°	1.538°
Homo sapiens	10.154°	6.772°	7.918°
Homo sapiens	0.64°	1.74°	1.966°
Homo sapiens	0.166°	0.773°	1.292°

Homo sapiens	0.6°	3.384°	2.355°
Homo sapiens	2.085°	0.924°	1.573°
Homo sapiens	2.445°	0.879°	1.249°
Homo sapiens	2.991°	1.281°	0.756°
Homo sapiens	0°	0°	1.078°
Homo sapiens	3.345°	1.166°	2.082°
Homo sapiens	2.971°	3.567°	3.93°
Homo sapiens	2.422°	5.586°	4.05°
Homo sapiens	10.467°	9.462°	8.243°
Homo sapiens	9.759°	10.87°	9.462°
Homo sapiens	10.193°	8.489°	10.249°
Homo sapiens	3.18°	2.27°	0.648°
Homo sapiens	0.633°	1.909°	0.499°
Homo sapiens	12.066°	9.942°	8.287°
Homo sapiens	7.06°	5.1°	6.943°
Homo sapiens	0.412°	1.277°	0.467°
Homo sapiens	0.697°	1.76°	2.413°
Homo sapiens	4.905°	6.697°	7.253°
Homo sapiens	8.489°	6.132°	7.155°
Homo sapiens	4.653°	2.09°	5.44°
Homo sapiens	4.671°	5.785°	6.695°
Homo sapiens	13.134°	11.877°	11.944°
Homo sapiens	0.245°	1.944°	2.592°
Homo sapiens	6.301°	6.468°	4.181°
Homo sapiens	1.665°	5.485°	3.33°
Homo sapiens	4.639°	1.481°	3.166°
Homo sapiens	3.501°	4.793°	2.072°
Homo sapiens	2.61°	0°	1.716°
Homo sapiens	2.441°	0.167°	1.105°
Homo sapiens	0.61°	0.643°	0°
Homo sapiens	2.379°	0°	1.54°
Homo sapiens	3.638°	0.732°	1.107°
Homo sapiens	3.576°	1.498°	1.823°
Homo sapiens	1.41°	0°	1.49°
Homo sapiens	1.584°	3.209°	1.063°
Homo sapiens	0.814°	2.472°	3.076°
Homo sapiens	3.489°	4.59°	1.02°
Homo sapiens	11.842°	4.938°	7.76°
Homo sapiens	5.637°	5.406°	5.492°
Homo sapiens	10.62°	12.187°	12.698°
Homo sapiens	5.859°	5.227°	5.634°
Homo sapiens	5.29°	6.367°	6.285°
Homo sapiens	3.31°	5.097°	5.387°
Homo sapiens	2.694°	4.487°	4.657°
Homo sapiens	2.679°	3.347°	1.412°
Homo sapiens	8.722°	9.055°	9.296°

Homo sapiens	10.965°	12.011°	11.986°
Homo sapiens	10.064°	10.7°	7.202°
Homo sapiens	3.826°	4.608°	2.9°
Homo sapiens	6.176°	7.584°	6.78°
Homo sapiens	0.644°	4.909°	6.219°
Homo sapiens	11.518°	15.415°	16.189°
Homo sapiens	14.231°	15.518°	17.182°
Homo sapiens	0.46°	0.966°	0.268°
Homo sapiens	2.888°	1.825°	0.156°
Homo sapiens	6.998°	10.216°	9.529°
Homo sapiens	0.741°	0.402°	0.405°
Homo sapiens	2.987°	2.759°	1.848°
Homo sapiens	4.781°	3.827°	3.386°
Homo sapiens	2.61°	4.485°	5.481°
Homo sapiens	3.147°	3.845°	5.28°
Homo sapiens	4.086°	4.683°	5.238°
Homo sapiens	7.331°	6.746°	4.467°
Homo sapiens	7.604°	4.97°	3.992°
Homo sapiens	4.399°	4.864°	6.661°
Homo sapiens	5.141°	4.889°	6.83°
Homo sapiens	5.181°	7.186°	4.154°
Homo sapiens	3.229°	3.039°	5.01°
Homo sapiens	2.529°	2.222°	2.012°
Homo sapiens	6.934°	9.337°	7.788°
Homo sapiens	10.864°	6.934°	7.34°
Homo sapiens	9.926°	7.534°	7.934°
Homo sapiens	16.765°	13.963°	13.927°
Homo sapiens	15.376°	13.321°	15.054°
Homo sapiens	6.511°	0.501°	1.718°
Homo sapiens	0.085°	2.981°	1.361°
Homo sapiens	5.517°	3.082°	4.109°
Homo sapiens	13.03°	15.969°	15.667°
Homo sapiens	2.42°	3.945°	3.888°
Homo sapiens	2.667°	5.097°	4.22°
Homo sapiens	14.258°	12.106°	13.167°
Homo sapiens	16.334°	15.327°	14.708°
Homo sapiens	0.815°	4.669°	2.429°
Homo sapiens	0.693°	2.716°	3.219°
Pan troglodytes	37.036°	32.692°	33.465°
Pan trogodytes	11.13°	13.081°	13.987°
Pan troglodytes	11.497°	15.0347°	13.476°
Pan troglodytes	22.294°	26.64°	24.736°
Pan troglodytes	16.327°	15.54°	14.889°
Pan troglodytes	27.525°	27.626°	25.525°
Pan troglodytes	16.109°	20.635°	15.346°
Pan troglodytes	26.837°	30.382°	26.565°

Gorilla gorilla	25.626°	25.58°	25.201°
Gorilla gorilla	28.179°	29.418°	29.851°
Gorilla gorilla	19.97°	20.141°	19.747°
Gorilla gorilla	24.274°	25.734°	26.755°
Gorilla gorilla	28.691°	28.667°	31.343°
Gorilla gorilla	23.454°	22.759°	22.116°
Hylobates lar	18.172°	22.985°	25.033°
Hylobates lar	28.196°	25.244°	25.768°
Hylobates lar	23.741°	26.707°	24.215°
Hylobates lar	15.583°	14.916°	14.583°
Hylobates lar	4.675°	10.516°	6.719°
Hylobates lar	22.642°	23.358°	23°
Hylobates lar	16.538°	15.104°	19.523°
Hylobates lar	8.427°	7.616°	6.128°
Hylobates lar	28.432°	25.287°	25.274°
Hylobates lar	26.565°	25.463°	26.311°
Hylobates lar	27.619°	28.278°	27.364°
Hylobates lar	24.102°	22.891°	23.035°
Hylobates lar	22.852°	21.94°	22.006°
Hylobates lar	30.245°	34.563°	34.592°
Hylobates lar	19.536°	22.951°	24.882°
Symphalangus syndactylus	18.902°	17.398°	18.387°
Symphalangus syndactylus	21.146°	22.689°	21.982°
Symphalangus syndactylus	17.459°	19.058°	17.056°
Symphalangus syndactylus	21.187°	19.51°	23.555°
Symphalangus syndactylus	28.757°	28.122°	27.262°
Symphalangus syndactylus	27.824°	29.163°	30.33°
Symphalangus syndactylus	32.362°	30.152°	33.155°
Symphalangus syndactylus	34.472°	32.735°	35.446°
Symphalangus syndactylus	18.159°	21.443°	20.35°
Symphalangus syndactylus	24.42°	28.894°	29.187°
Papio ursinus	12.605°	14.721°	12.996°
Papio ursinus	10.219°	8.572°	7.534°
Papio ursinus	10.164°	10.835°	11.83°
Papio ursinus	5.728°	4.511°	1.252°
Papio ursinus	0.616°	1.348°	3.202°
Papio ursinus	5.37°	7.326°	6.937°
Papio ursinus	4.475°	6.429°	5.912°
Papio ursinus	0.93°	8.259°	9.139°
Papio ursinus	12.913°	12.441°	12.413°
Papio ursinus	4.399°	5.778°	5.194°
Papio ursinus	9.067°	8.034°	0.756°
Papio ursinus	3.915°	0.415°	1.521°
Papio ursinus	8.288°	5.675°	8.055°
Papio ursinus	19.946°	18.864°	17.923°
Papio ursinus	17.674°	16.918°	17.978°

Papio ursinus	5.389°	2.02°	2.808°
Papio ursinus	4.656°	2.779°	6.229°
Papio ursinus	2.458°	5.08°	7.291°
Papio ursinus	2.515°	0.592°	0.174°
Papio ursinus	21.762°	21.4°	21.981°
Papio ursinus	2.261°	4.1°	1.193°
Papio ursinus	9.802°	9.025°	9.435°
Papio ursinus	8.641°	8.885°	7.853°
Papio ursinus	8.881°	2.447°	8.629°
Papio ursinus	7.872°	8.893°	8.973°
Papio ursinus	6.134°	6.258°	10.147°
Papio ursinus	14.353°	11.026°	17.199°
Papio ursinus	2.689°	7.294°	7.663°
Papio ursinus	6.82°	0.224°	6.733°
Papio ursinus	0.34°	0.419°	2.571°
Papio ursinus	12.605°	11.08°	9.134°
Papio ursinus	5.728°	5.589°	5.801°
Papio ursinus	7.595°	6.789°	7.584°
Papio ursinus	5.37°	0°	0.174°
Papio ursinus	4.475°	2.417°	5.21°
Papio ursinus	14.381°	14.759°	16.365°
Papio ursinus	8.099°	7.663°	7.693°
Papio ursinus	18.017°	15.124°	14.673°
Papio ursinus	1.723°	3.969°	3.988°
Papio ursinus	2.905°	4.764°	6.603°
Papio ursinus	6.68°	9.462°	8.596°
Papio ursinus	16.161°	14.392°	15.136°
Papio ursinus	10.228°	9.62°	10.026°
Papio ursinus	2.066°	3.639°	3.038°
Papio ursinus	7.204°	5.654°	6.165°
Papio ursinus	12.23°	6.694°	9.101°
Papio ursinus	6.054°	5.303°	5.906°
Papio ursinus	3.736°	4.312°	4.219°
Papio ursinus	0.436°	1.089°	2.804°
Papio ursinus	5.793°	7.444°	7.779°
Papio ursinus	7.779°	8.091°	10.396°
Papio ursinus	12.875°	14.498°	12.015°
Papio ursinus	2.242°	3.289°	2.802°
Papio ursinus	0.547°	0°	0°
Papio ursinus	0.169°	1.234°	0°
Papio ursinus	1.532°	0.714°	1.532°
Papio ursinus	8.746°	10.485°	11.077°
Papio ursinus	9.462°	8.746°	7.195°
Papio ursinus	0.159°	1.526°	2.374°
Papio cynocephalus	23.229°	20.514°	21.224°
Papio cynocephalus	23.229°	20.514°	21.224°

Papio cynocephalus	18.194°	17.669°	18.304°
Papio cynocephalus	21.801°	18.268°	19.497°
Papio cynocephalus	21.839°	19.708°	19.805°
Papio cynocephalus	18.166°	19.455°	19.029°
Papio cynocephalus	16.372°	17.678°	17.482°
Papio cynocephalus	18.638°	16.377°	17.934°
Papio cynocephalus	18.538°	17.696°	17.061°
Papio cynocephalus	15.276°	15.491°	14.4°
Papio cynocephalus	20.523°	17.946°	17.784°
Papio cynocephalus	12.6°	10.886°	9.598°
Papio cynocephalus	7.102°	5.951°	6.649°
Papio cynocephalus	16.99°	15.023°	11.952°
Papio cynocephalus	18.939°	15.046°	17.934°
Papio cynocephalus	16.999°	15.232°	12.391°
Papio cynocephalus	5.899°	7.217°	8.842°
Papio cynocephalus	6.483°	4.553°	8.64°
Papio cynocephalus	6.134°	7.629°	6.911°
Papio cynocephalus	6.034°	5.575°	6.65°
Papio cynocephalus	6.34°	5.602°	5.434°
Papio cynocephalus	7.93°	9.201°	7.251°
Papio cynocephalus	5.225°	6.811°	5.809°
Papio cynocephalus	5.117°	6.667°	6.371°
Papio cynocephalus	4.919°	3.933°	3.489°
Papio cyanocephalus	2.695°	4.783°	4.544°
Papio cyanocephalus	13.771°	14.191°	15.997°
Papio hamadryas	7.269°	11.921°	12.619°
Papio hamadryas	5.64°	6.378°	5.16°
Papio hamadryas	7.912°	11.83°	5.315°
Papio hamadryas	6.71°	5.098°	2.209°
Papio hamadryas	1.219°	3.108°	1.209°
Papio hamadryas	0.457°	4.882°	0.434°
Papio hamadryas	2.774°	1.558°	0°
Papio hamadryas	1.975°	3.519°	5.207°
Papio hamadryas	3.627°	2.549°	3.991°
Papio hamadryas	1.253°	2.305°	0.348°
Papio hamadryas	0.641°	4.559°	4.557°
Papio hamadryas	0.929°	0.901°	0.234°
Papio hamadryas	4.764°	1.79°	3.761°
Papio hamadryas	4.011°	2.921°	3.221°
Papio hamadryas	11.046°	10.594°	9.248°
Papio hamadryas	13.319°	11.502°	9.693°
Papio hamadryas	9.369°	12.688°	11.54°
Papio hamadryas	9.595°	6.95°	8.768°
Papio hamadryas	9.694°	6.778°	8.514°
Papio hamadryas	13.901°	12.721°	13.861°
Papio hamadryas	6.054°	4.049°	2.904°

Papio hamadryas	3.908°	4.955°	5.423°
Papio hamadryas	8.332°	8.34°	7.863°
Papio hamadryas	11.232°	15.852°	14.519°
Papio hamadryas	10.008°	11.424°	11.747°
Papio hamadryas	13.312°	9.406°	11.011°
Lophocebus atterhimus	16.431°	17.228°	17.914°
Lophocebus atterhimus	18.362°	15.117°	14.158°
Lophocebus atterhimus	16.584°	12.928°	16.348°
Lophocebus atterhimus	21.894°	21.705°	22.338°
Papio hamadryas	12.105°	13.449°	12.339°
Mandrillus sphinx	24.503°	24.837°	23.367°
Mandrillus sphinx	14.767°	17.459°	16.054°
Mandrillus sphinx	12.758°	17.268°	17.659°
Mandrillus sphinx	16.043°	11.796°	14.469°
Mandrillus sphinx	19.689°	15.446°	14.826°
Mandrillus sphinx	21.151°	21.592°	22.273°
Mandrillus leucophaeus	26.135°	23.872°	24.567°
Mandrillus leucophaeus	26.775°	24.85°	25.201°
Mandrillus leucophaeus	24.112°	24.572°	25.08°
Mandrillus leucophaeus	25.665°	24.711°	22.455°
Mandrillus leucophaeus	24.413°	25.897°	25.683°
Mandrillus leucophaeus	26.889°	24.575°	25.321°
Mandrillus leucophaeus	26.136°	25.427°	23.814°
Mandrillus leucophaeus	28.535°	27.842°	25.297°
Mandrillus leucophaeus	27.832°	25.816°	26.042°
Mandrillus leucophaeus	28.091°	26.263°	25.762°
Mandrillus leucophaeus	28.518°	27.165°	28.173°
Mandrillus leucophaeus	28.488°	28.224°	26.565°
Mandrillus leucophaeus	31.989°	31.683°	32.687°
Macaca silenus	2.055°	4.002°	0.315°
Macaca silenus	18.392°	17.14°	17.557°
Macaca silenus	15.077°	14.814°	15.225°
Macaca silenus	12.607°	15.048°	13.118°
Macaca silenus	16.47°	16.656°	16.436°
Macaca silenus	17.103°	18.728°	19.775°
Macaca silenus	14.632°	13.551°	12.431°
Cercopithecus neglectus	20.395°	16.157°	15.18°
Cercopithecus neglectus	24.945°	22.893°	21.434°
Cercopithecus neglectus	20.459°	20.556°	22.348°
Cercopithecus neglectus	23.029°	22.856°	23.714°
Cercopithecus neglectus	16.015°	17.624°	18.619°
Cercopithecus neglectus	8.588°	7.889°	7.817°
Cercopithecus neglectus	15.499°	13.021°	12.168°
Cercopithecus neglectus	19.161°	18.837°	17.518°
Cercopithecus neglectus	22.951°	22.598°	22.181°
Cercopithecus neglectus	20.014°	21.176°	21.249°

Cercopithecus mona	26.653°	25.56°	26.072°
Cercopithecus mona	25.005°	24.775°	27.036°
Cercopithecus mona	14.424°	13.403°	14.676°
Cercopithecus mona	12.655°	12.003°	15.391°
Cercopithecus mona	14.158°	15.894°	16.426°
Cercopithecus mona	21.265°	17.745°	18.853°
Cercopithecus mona	17.103°	20.335°	22.008°
Cercopithecus mona	6.71°	4.399°	7.731°
Cercopithecus mona	13.668°	14.612°	17.503°
Cercopithecus mona	14.831°	16.474°	16.39°
Cercopithecus mona	18.631°	22.026°	18.559°
Cercopithecus mona	25.645°	24.52°	24.088°
Cercopithecus mona	17.343°	22.084°	25.57°
Cercopithecus mona	19.465°	19.162°	18.001°
Cercopithecus mona	20.056°	17.275°	17.853°
Cercopithecus ascanius	20.785°	18.992°	22.473°
Cercopithecus ascanius	31.342°	32.005°	30.474°
Cercopithecus diana	21.86°	24.84°	23.42°
Cercopithecus diana	7.64°	7.5°	7.09°
Cercopithecus diana	24.91°	22.5°	21.77°
Cercopithecus diana	21.45°	23.47°	25.67°
Cercopithecus diana	20.48°	22.01°	43.65°
Cercopithecus diana	23.88°	25.76°	24.36°
Cercopithecus diana	22°	23.36°	26.17°
Cercopithecus diana	28.8°	30.15°	29.42°
Cercopithecus diana	17.1°	11.99°	8.92°
Cercopithecus diana	24.62°	26.87°	28.22°
Chlorocebus pygerythrus	20.505°	23.279°	19.718°
Colobus guereza	18.61°	22.778°	18.435°
Colobus guereza	29.859°	30.824°	31.78°
Colobus guereza	28.329°	27.001°	28.74°
Colobus guereza	30.374°	30.24°	28.73°
Colobus guereza	26.267°	25.081°	24.859°
Colobus guereza	30.036°	30.448°	30.915°
Colobus guereza	31.82°	30.141°	31.284°
Colobus guereza	29.975°	27.939°	28.878°
Colobus guereza	32.33°	35.083°	35.577°
Colobus guereza	34.101°	35.455°	35.319°
Colobus guereza	15.661°	12.944°	13.856°
Colobus guereza	22.206°	20.256°	21.801°
Colobus guereza	21.194°	21.187°	20.36°
Colobus guereza	22.555°	23.145°	22.999°
Colobus guereza	21.847°	22.769°	22.971°
Colobus guereza	15.969°	16.515°	15.803°
Chlorocebus pygerythrus	19°	23.279°	23.097°
Chlorocebus pygerythrus	21.976°	26.947°	24.193°

Chlorocebus pygerythrus	21.837°	24.842°	21.872°
Chlorocebus pygerythrus	20.966°	26.667°	24.979°
Chlorocebus pygerythrus	24.121°	19.822°	22.422°
Chlorocebus pygerythrus	21.371°	25.586°	22.6°
Chlorocebus pygerythrus	17.536°	14.612°	14.641°
Lemur catta	24.672°	24.17°	22.495°
Lemur catta	30.619°	27.89°	29.71°
Lemur catta	25.852°	28.235°	30.763°
Lemur catta	21.495°	21.697°	19.523°
Lemur catta	16.319°	19.654°	19.928°
Lemur catta	21.438°	20.404°	19.73°
Lemur catta	24.075°	22.999°	21.604°
Lemur catta	34.674°	34.224°	34.885°
Lemur catta	30.111°	32.002°	33.558°
Lemur catta	18.375°	17.585°	19.569°
Lemur catta	32.307°	30.196°	31.888°
Lemur catta	28.61°	27.532°	29.038°
Eulemur coranatus	32.4°	29.3°	33.3°
Eulemur coranatus	20.1°	14.0°	17.1°
Eulemur coranatus	17.1°	12.0°	11.7°
Eulemur coranatus	11.3°	12.4°	11.5°
Eulemur coranatus	34.8°	36.3°	35.5°
Eulemur coranatus	37.3°	34.2°	33.9°
Eulemur coranatus	37.6°	37.2°	33.7°
Eulemur coranatus	1.81°	6.70°	6.34°
Eulemur coranatus	32.8°	32.0°	31.0°
Varecia variegata	21.624°	22.682°	23.234°
Varecia variegata	27.806°	27.845°	28.963°
Varecia variegata	26.686°	28.452°	28.978°
Varecia variegata	30.76°	35.548°	32.922°
Varecia variegata	29.219°	32.368°	32.719°
Varecia variegata	29.285°	31.307°	31.334°
Callithrix jacchus	26.728°	23.687°	24.834°
Callithrix jacchus	31.659°	32.912°	32.415°
Callithrix jacchus	10.869°	8.621°	9.634°
Callithrix jacchus	11.757°	9.308°	12.197°

Table 3: Mean values calculated from the specimens used in this study. NH = Neutral head posture, LCO = Lateral canal orientation, LDI = Locomotor diversity index. LDI for *Lophocebus atterhimus* is taken from closely related *Lophocebus albigena* Values for LDI and Locomotor mode are from Granatosky (2018).ML = Main locomotor mode (1 = Bipedalism, 2 = knuckle walking, 3 = emaciation, 4 = arboreal quadrupedalism, 5 = terrestrial quadrupedalism, 6 = vertical climber) All values are log-transformed using a natural logarithm. Masses are in grams.

Taxon	ln(NH)	ln(LCO)	Ln(Body mass)	ln(Brain mass)	LDI	LM
Homo sapiens	1.63	3.08	11.18	7.19	-	1
Australopithecus africanus	-	3.28	8.13	6.12	-	-
Pan troglodytes	3.07	3.17	10.87	5.88	04	2
Gorilla gorilla	3.24	3.19	11.7	6.21	0.18	2
Hylobates lar	3.07	2.96	8.67	4.62	1.11	3
Symphalangus syndactylus	3.22	3.01	9.33	4.86	0.79	3
Papio angusticeps	-	2.98	8	-	-	-
Dinopithecus ingens		3.04	8.43	4.77	-	4
Parapapio jonesi	-	3.03	7.31	4.75	-	-
Parapapio whitei	-	2.98	7.54	5.03	-	-
Papio ursinus	1.97	2.92	10.01	5.13	-	4
Papio cynocephalus	2.55	2.84	9.75	5.02	-	4
Papio hamadryas	1.91	2.82	9.56	4.94	-	4
Lophocebus aterrimus	2.87	3.13	8.83	4.69	1.15	5
Mandrillus sphinx	2.9	3.02	10.07	5.05	-	4
Mandrillus leucophaeus	3.27	3.26	9.62	4.82	-	4
Macaca silenus	2.63	3.19	8.92	4.44	-	4
Cercopithecus neglectus	2.92	3.08	8.6	4.23	-	5
Cercopithecus mona	3.31	3.3	8.22	4.15	-	5
Cercopithecus ascanius	3.26	3.3	8.22	4.12	1.3	5
Cercopithecus diana	3.11	3	8.74	4.18	1.11	5
Chlorocebus pygerythrus	3.09	3.12	8.37	4.14	1.77	4
Colobus guereza	3.25	3.19	9.06	4.29	1.37	5
Cercopithecoides williamsi	-	2.98	9.9	5.17	-	4
Lemur catta	3.25	3.11	7.7	3.13	1.35	4
Eulemur coronatus	3.22	3.44	7.07	3.09	1.3	5
Varecia variegata	3.38	3.34	8.18	3.41	1.3	5
Callithrix jacchus	2.97	1.85	5.77	2.05	-	6

Table 4: Coefficient of variation (% error) of 10 LSCC orientation measurements (5 on each ear) of two specimens. SD = Standard deviation.

***Pan troglodytes* AG-06**	***Papio ursinus*** **sbu: RS PU-E**
21.5°	17.3°
21.7°	17.5°
22.0°	20.9°
21.9°	17.00°
19.00°	20.3°
23.1°	14.00°
23.3°	15.2°
23.8°	13.00°
24.0°	14.5°
22.3°	15.1°
SD = 1.4	**SD** = 2.6
% error = 6%	**% error** =16%

Table 5: Randomly selected sets of measurements of neutral head postures taken from photos used to estimates the coefficient of variation (CV) in the measurement process. SD = Standard deviation.

Measurement 1	**Measurement 2**	**Measurement 3**	**SD**	**CV**
24.503	24.837	23.369	0.77	3%
12.607	15.048	13.118	1.28	9%
24.945	22.893	21.434	1.76	7%
16.319	19.654	19.928	0.77	8%
17.103	20.335	22.008	2.49	12%

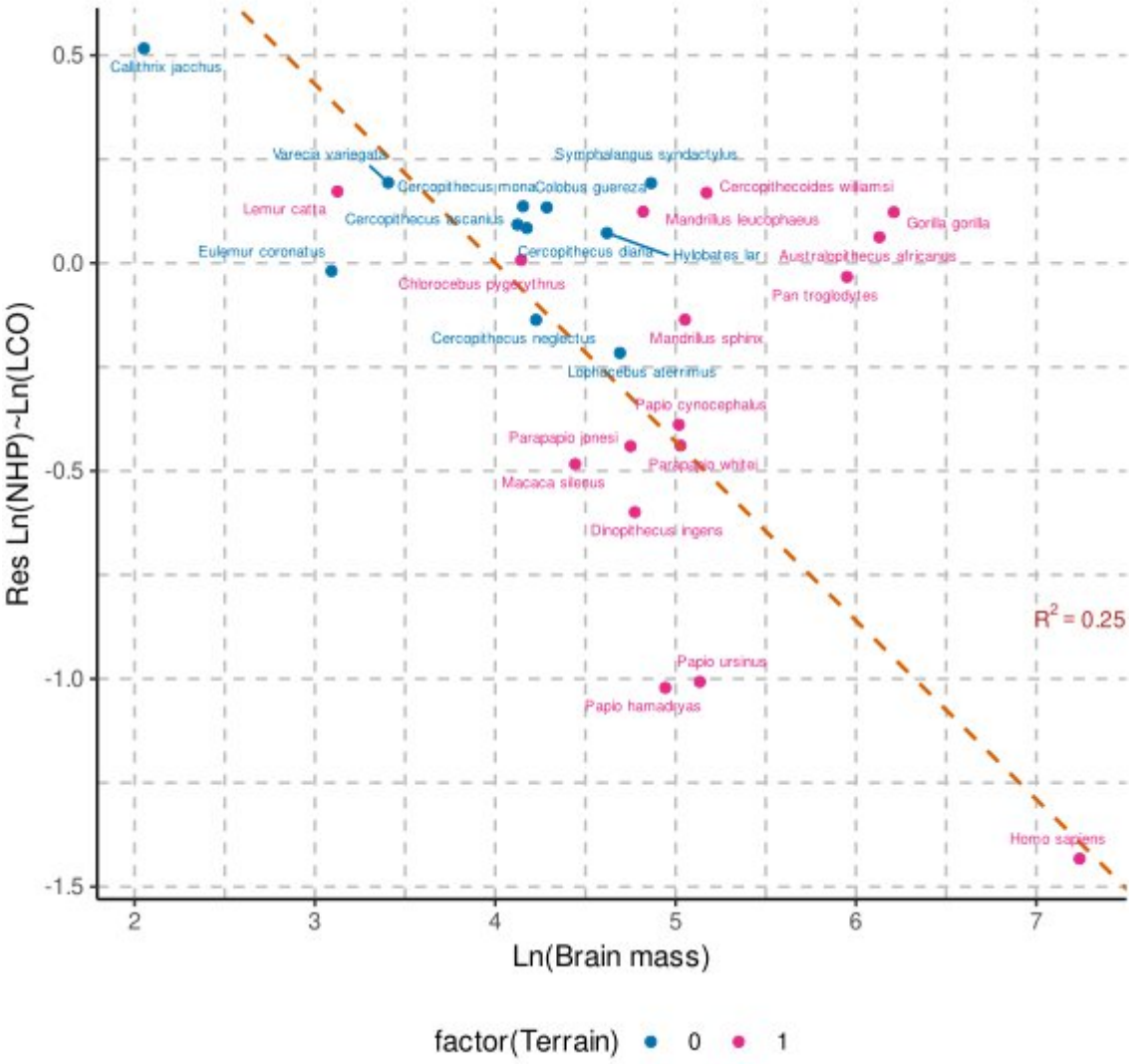

Figure 1. Residuals plot of Ln(Neutral head posture) v.s Ln(LSCC orientation) v.s Ln (Brain mass in grams). Species reconstructed as terrestrial and extant predominantly terrestrial species are in pink and predominantly arboreal species are in blue.

Table 7. LSC orientation v.s Ln(Brain mass) +Ln(Body mass) +Ln(Neutral head postures)+ Terrain (Arboreal and Terrestrial). * = significant at $p < 0.05$. Correlations are modelled under a Brownian motion model.

Coefficients	**Value**	**Std.Error**	**t-value**	**p-value**
(Intercept)	2.21	0.507	4.373	0.0002

Ln(Brain mass)	0.268	0.115	2.31	0.0300*
Ln(Body mass)	-0.102	0.052	-1.97	0.06
Ln(NHP)	0.192	0.101	1.899	0.07
Terrain	-0.090	0.110	-0.819	0.42

REFERENCES

Adams, J.W., Rovinsky, D.S., 2018. Taphonomic interpretations of the Haasgat HGD assemblage: A case study in the impact of sampling and preparation methods on reconstructing South African karstic assemblage formation. Quaternary International, In Honour of James Brink. 495, 4–18.

Angelaki, D.E., Cullen, K.E., 2008. Vestibular System: The Many Facets of a Multimodal Sense. Annual Review of Neuroscience. 31, 125–150.

Anthony, J., 1953. Justification des principes de la méthode véstibulaire. Mammalia. 17, 275–280.

Arnold, C., Matthews, L.J., Nunn, C.L., 2010. The 10kTrees website: A new online resource for primate phylogeny. Evolutionary Anthropology: Issues, News, and Reviews. 19, 114–118.

Bamford, M., 1999. Pliocene fossil woods from an early hominid cave deposit, Sterkfontein, South Africa. South African Journal of Science. 95, 231–237.

Bastir, M., Rosas, A., 2016. Cranial base topology and basic trends in the facial evolution of Homo. Journal of Human Evolution. 91, 26–35.

Bastir, M., Rosas, A., Kuroe, K., 2004. Petrosal orientation and mandibular ramus breadth: Evidence for an integrated petroso-mandibular developmental unit. American Journal of Physical Anthropology. 123, 340–350.

Bastir, M., Rosas, A., Stringer, C., Manuel Cuétara, J., Kruszynski, R., Weber, G.W., Ross, C.F., Ravosa, M.J., 2010. Effects of brain and facial size on basicranial form in human and primate evolution. Journal of Human Evolution. 58, 424–431.

Beaudet, A., 2015. Characterization of inner craniodental structures in cercopithecoids and diachronic study of their morphological variation in the Plio-pleistocene south African sequence (phd thesis). Université Paul Sabatier - Toulouse III.

Beaudet, A., Dumoncel, J., de Beer, F., Duployer, B., Durrleman, S., Gilissen, E., Hoffman, J., Tenailleau, C., Thackeray, J.F., Braga, J., 2016a. Morphoarchitectural variation in South African fossil cercopithecoid endocasts. Journal of Human Evolution. 101, 65–78.

Beaudet, A., Dumoncel, J., Thackeray, J.F., Bruxelles, L., Duployer, B., Tenailleau, C., Bam, L., Hoffman, J., de Beer, F., Braga, J., 2016b. Upper third molar internal structural organization and semicircular canal morphology in Plio-Pleistocene South African cercopithecoids. Journal of Human Evolution. 95, 104–120.

Beaudet, A., Gilissen, E., 2018. Fossil Primate Endocasts: Perspectives from Advanced Imaging Techniques. In: Bruner, E., Ogihara, N., Tanabe, H.C. (Eds.), Digital Endocasts: From Skulls to Brains, Replacement of Neanderthals by Modern Humans Series. Springer Japan, Tokyo, pp. 47–58.

Beaudet, A., Clarke, R.J., Bruxelles, L., Carlson, K.J., Crompton, R., de Beer, F., Dhaene, J., Heaton, J.L., Jakata, K., Jashashvili, T., Kuman, K., McClymont, J., Pickering, T.R., Stratford, D., 2019. The bony labyrinth of StW 573 (“Little Foot”): Implications for early hominin evolution and paleobiology. Journal of Human Evolution. 127, 67–80

Beaudet, A., Du, A., Wood, B., 2019. Evolution of the modern human brain. Progress in brain research. 250, 219–250.

Beaudet, A., Holloway, R., Benazzi, S., 2021. A comparative study of the endocasts of OH 5 and SK 1585: Implications for the paleoneurology of eastern and southern African Paranthropus. Journal of Human Evolution. 156, 103010.

Beaudet, A., 2023. The Australopithecus assemblage from Sterkfontein Member 4 (South Africa) and the concept of variation in palaeontology. Evolutionary Anthropology: Issues, News, and Reviews. n/a.

Beaulieu, J.M., Oliver, J.C., O'Meara, B. and Beaulieu, M.J., 2017. Package ‘corHMM’. *Analysis of Binary Character Evolution*.

Beer, D., 1947. PRESIDENTIAL ADDRESS: How Animals hold their Heads. Proceedings Linnean Society London. 159, 125–139.

Benson, R.B., Starmer-Jones, E., Close, R.A. and Walsh, S.A., 2017. Comparative analysis of vestibular ecomorphology in birds. *Journal of Anatomy*, *231*(6), pp.990-1018.

Biegert, J., 1957. Der Formwandel des Primatenschadels und seine Beziehungen zur ontogenetischen Entwicklung und den phylogenetischen Spezialisationen der Kopforgan. Morphol. Jahrb. 98, 77– 199.

Benoit, J., Legendre, L.J., Farke, A.A., Neenan, J.M., Mennecart, B., Costeur, L., Merigeaud, S., Manger, P.R., 2020. A test of the lateral semicircular canal correlation to head posture, diet and other biological traits in “ungulate” mammals. Scientific Reports. 10, 19602.

Benoit-Gonin, L., Lafite-Dupont, P., 1907. Destinée du canal semi-circulaire externe dans le passage de la station quadrupède à la station bipède. CR Soc. Biol. Paris. 62, 98–99.

Benson, R.B., Starmer-Jones, E., Close, R.A. and Walsh, S.A., 2017. Comparative analysis of vestibular ecomorphology in birds. Journal of Anatomy, 231(6), pp.990-1018.

Berger, L.R., Lacruz, R., De Ruiter, D.J., 2002. Revised age estimates of Australopithecus-bearing deposits at Sterkfontein, South Africa. American Journal of Physical Anthropology. 119, 192–197.

Berlin, J.C., Kirk, E.C., Rowe, T.B., 2013. Functional Implications of Ubiquitous Semicircular Canal Non-Orthogonality in Mammals. PLOS ONE. 8, e79585.

Bertrand, O.C., Püschel, H.P., Schwab, J.A., Silcox, M.T., Brusatte, S.L., 2021. The impact of locomotion on the brain evolution of squirrels and close relatives. Communications Biology. 4, 1–15.

Biegert, J., 1957. Der Formwandel des Primatenschadels und seine Beziehungen zur ontogenetischen Entwicklung und den phylogenetischen Spezialisationen der Kopforgan. Morphol. Jahrb. 98, 77– 199.

Biegert, J., 1963. The evolution of characteristics of the skull, hands, and feet. Classification and Human Evolution. 116–145.

Birchette, M.G., 1982. The postcranial skeleton of Paracolobus chemeroni. Harvard University.

Blanks, R., Curthoys, I., Markham, C., 1975. Planar relationships of the semicircular canals in man. Acta oto-laryngologica. 80, 185–196.

Blanks, R.H.I., Curthoys, I.S., Bennett, M.L., Markham, C.H., 1985. Planar relationships of the semicircular canals in rhesus and squirrel monkeys. Brain Research. 340, 315–324.

Blomberg, S.P., Garland Jr, T., Ives, A.R., 2003. Testing for phylogenetic signal in comparative data: behavioural traits are more labile. Evolution. 57, 717–745.

Bobe, R., Behrensmeyer, A.K., 2004. The expansion of grassland ecosystems in Africa in relation to mammalian evolution and the origin of the genus Homo. Palaeogeography, Palaeoclimatology, Palaeoecology, Evolution of grass-dominated ecosystems during the late Cenozoic Session at the North American Paleontological Convention, 2001. 207, 399–420.

Boyle, E.K., McNutt, E.J., Sasaki, T., Suwa, G., Zipfel, B., DeSilva, J.M., 2018. A quantification of calcaneal lateral plantar process position with implications for bipedal locomotion in Australopithecus. Journal of Human Evolution. 123, 24–34.

Boddy, A.M., McGOWEN, M.R., Sherwood, C.C., Grossman, L.I., Goodman, M., Wildman, D.E., 2012. Comparative analysis of encephalization in mammals reveals relaxed constraints on anthropoid primate and cetacean brain scaling. Journal of Evolutionary Biology. 25, 981–994.

Boyer, D.M., Gunnell, G.F., Kaufman, S., McGeary, T.M., 2016. Morphosource: Archiving and sharing 3-d digital specimen data. The Paleontological Society Papers. 22, 157–181.

Bronzati, M., Benson, R.B., Evers, S.W., Ezcurra, M.D., Cabreira, S.F., Choiniere, J., Dollman, K.N., Paulina-Carabajal, A., Radermacher, V.J., Roberto-da-Silva, L., 2021. Deep evolutionary diversification of semicircular canals in archosaurs. Current Biology. 31, 2520–2529.

Bull, J.W.D., 1969. Tentorium Cerebelli. Proceedings of the Royal Society of Medicine. 62, 1301–1310.

Bullar, C.M., Zhao, Q., Benton, M.J., Ryan, M.J., 2019. Ontogenetic braincase development in Psittacosaurus lujiatunensis (Dinosauria: Ceratopsia) using micro-computed tomography. PeerJ. 7, e7217.

Cant, J.G., 1992. Positional behavior and body size of arboreal primates: a theoretical framework for field studies and an illustration of its application. American journal of physical anthropology. 88, 273–283.

Chattergee, H.J., Ho, S.Y., Barnes, I. and Groves, C., 2009. Estimating the phylogeny and divergence

times of primates using a supermatrix approach. BMC evolutionary biology, 9, pp. 1-19.

Ciochon, R.L., 1993. Evolution of the cercopithecoid forelimb: phylogenetic and functional implications from morphometric analyses. University of California Press.

Coutier, F., Hautier, L., Cornette, R., Amson, E., Billet, G., 2017. Orientation of the lateral semicircular canal in Xenarthra and its links with head posture and phylogeny. Journal of Morphology. 278, 704–717.

Codron, D., Luyt, J., Lee, -Thorp Julia A., Sponheimer, M., De, R.D., Codron, J., 2005. Utilization of savanna-based resources by Plio-Pleistocene baboons : research letter. South African Journal of Science. 101, 245–248.

Cofran, Z., 2019. Brain size growth in Australopithecus. Journal of Human Evolution. 130, 72–82.

Crompton, R.H., McClymont, J., Elton, S., Thorpe, S., Sellers, W., Heaton, J., Pickering, T.R., Pataky, T., Carlson, K.J., Jashashvili, T., Beaudet, A., Bruxelles, L., Goh, E., Kuman, K., Clarke, R., 2021. StW 573 Australopithecus prometheus: Its Significance for an Australopith Bauplan. Folia Primatologica. 92, 243–275.

Cullen, K.E., 2012. The vestibular system: multimodal integration and encoding of self-motion for motor control. Trends in Neurosciences. 35, 185–196.

David, R., Droulez, J., Allain, R., Berthoz, A., Janvier, P., Bennequin, D., 2010. Motion from the past. A new method to infer vestibular capacities of extinct species. Comptes Rendus Palevol, Imaging & 3D in palaeontology and palaeoanthropology. 9, 397–410.

Day, M.H., Wickens, E.H., 1980. Laetoli Pliocene hominid footprints and bipedalism. Nature. 286, 385–387.

Day, B.L., Marsden, J.F., Ramsay, E., Mian, O.S., Fitzpatrick, R.C., 2010. Non-linear vector summation of left and right vestibular signals for human balance. The Journal of Physiology. 588, 671–682.

de Beer, G.R., 1947. PRESIDENTIAL ADDRESS: How Animals hold their Heads. Proceedings Linnean Society London. 159, 125–139.

DeSilva, J.M., Holt, K.G., Churchill, S.E., Carlson, K.J., Walker, C.S., Zipfel, B., Berger, L.R., 2013. The lower limb and mechanics of walking in Australopithecus sediba. Science. 340, 1232999.

de Sousa, A., Cunha, E., 2012. Chapter 14 - Hominins and the emergence of the modern human brain. In: Hofman, M.A., Falk, D. (Eds.), Progress in Brain Research, Evolution of the Primate Brain. Elsevier, pp. 293–322.

Dean, M.C., 1988. Growth processes in the cranial base of hominoids and their bearing on morphological similarities that exist in the cranial base of Homo and Paranthropus. In: Evolutionary History of the “Robust” Australopithecines. Aldine de Gruyter New York, pp. 107–112. Deaner, R.O., Isler, K., Burkart, J., Schaik, C. van, 2007. Overall Brain Size, and Not Encephalization

Quotient, Best Predicts Cognitive Ability across Non-Human Primates. Brain, Behavior and Evolution. 70, 115–124.

Delattre, A., Anthony, J., 1951. Les particularités cranio-encéphaliques du Saïmiri. Bulletins et Mémoires de la Société d'Anthropologie de Paris. 2, 166–176.

Delattre, A., Fenart, R., 1957a. La rotation du rocher, son mécanisme, ses conséquences sur les surfaces osseuses de voisinage. Bulletins et Mémoires de la Société d'Anthropologie de Paris. 8, 142–160.

Delattre, A., Fenart, R., 1958. Essai de systématisation du pariétal ; son utilisation au cours de l'étude de sa croissance. Bulletins et Mémoires de la Société d'Anthropologie de Paris. 9, 245–295.

Delattre, A., Fenart, R., 1960. L'hominisation du crâne: étudiée par la méthode vestibulaire. Éditions du Centre national de la recherche scientifique

Delattre, A., Fenart, R., 1961. Evolution des fenêtres du vestibule des mammifères a l'homme. Bulletins et Mémoires de la Société d'Anthropologie de Paris. 2, 273–289.

Delattre, A., Fenart, R., 1962. Note sur l'étude du crâne, en projections vestibulaires horizontales et frontales. Bulletins et Mémoires de la Société d'Anthropologie de Paris. 3, 439–443.

Delson, E., 2017. Toward the origin of the Old World monkeys. In: Primate Evolution and Human Origins. Routledge, pp. 175–181.

Delson, E., Andrews, P., 1975. Evolution and interrelationships of the catarrhine primates.

In: Phylogeny of the Primates. Springer, pp. 405–446.

Delson, E., Terranova, C.J., Jungers, W.L., Sargis, E.J., Jablonski, N.G., 2000. Body mass in Cercopithecidae (Primates, Mammalia): estimation and scaling in extinct and extant taxa.

Anthropological papers of the AMNH; no. 83.

Dembo, M., Radovčić, D., Garvin, H.M., Laird, M.F., Schroeder, L., Scott, J.E., Brophy, J., Ackermann, R.R., Musiba, C.M., de Ruiter, D.J., 2016. The evolutionary relationships and age of Homo naledi: An assessment using dated Bayesian phylogenetic methods. Journal of Human Evolution. 97, 17–26.

DeVore, I., Washburn, S., L., 1963. Baboon Ecology and Human Evolution. African Ecology and Human Evolution. 36, 335

Du, A., Zipkin, A.M., Hatala, K.G., Renner, E., Baker, J.L., Bianchi, S., Bernal, K.H., Wood, B.A., 2018. Pattern and process in hominin brain size evolution are scale-dependent. Proceedings of the Royal Society B: Biological Sciences. 285, 20172738.

Elton, S., 2000. Ecomorphology and evolutionary biology of African cercopithecoids: providing an ecological context for hominin evolution.

Elton, S., 2001a. Locomotor and habitat classifications of cercopithecoid postcranial material from Sterkfontein member 4, Bolt's Farm and Swartkrans Members 1 and 2, South Africa. KIP Articles.

Elton, S., 2001b. Locomotor and habitat classifications of cercopithecoid postcranial material from Sterkfontein member 4, Bolt's Farm and Swartkrans Members 1 and 2, South Africa. KIP Articles.

Elton, S., 2007. Environmental correlates of the cercopithecoid radiations. Folia Primatologica. 78, 344–364. Elton, S., Dunn, J., 2020. Baboon biogeography, divergence, and evolution: Morphological and paleoecological perspectives. Journal of Human Evolution. 145, 10279

Evers, S.W., Joyce, W.G., Choiniere, J.N., Ferreira, G.S., Foth, C., Hermanson, G., Yi, H., Johnson, C.M., Werneburg, I., Benson, R.B.J., 2022. Independent origin of large labyrinth size in turtles.

Nature Communications. 13, 5807.

Faith, J.T., Du, A., Behrensmeyer, A.K., Davies, B., Patterson, D.B., Rowan, J., Wood, B., 2021. Rethinking the ecological drivers of hominin evolution. Trends in Ecology & Evolution. 36, 797–807.

Ferreira, T. and Rasband, W., 2012. Setting measurements. In ImageJ user guide.

Fetter, M., Hain, T., Zee, D., 1986. Influence of eye and head position on the vestibulo-ocular reflex. Experimental brain research. 64, 208–216.

Fitzpatrick, R.C., Butler, J.E., Day, B.L., 2006. Resolving Head Rotation for Human Bipedalism. Current Biology. 16, 1509–151.

Fourie, N.H., Lee-Thorp, J.A., Ackermann, R.R., 2008. Biogeochemical and craniometric investigation of dietary ecology, niche separation, and taxonomy of Plio-Pleistocene cercopithecoids from the Makapansgat Limeworks. American Journal of Physical Anthropology: The Official Publication of the American Association of Physical Anthropologists. 135, 121–135.

Freimann, F.B., Luhdo, M.L., Rohde, V., Vajkoczy, P., Wolf, S. and Sprung, C., 2014. The Frankfurt horizontal plane as a reference for the implantation of gravitational units: a series of 376 adult patients. Acta neurochirurgica, 156, pp.1351-1356.

Frost, S.R., Delson, E., 2002. Fossil Cercopithecidae from the Hadar Formation and surrounding areas of the Afar Depression, Ethiopia. Journal of Human Evolution. 43, 687–748.

Gilbert, C.C., Steininger, C.M., Kibii, J.M., Berger, L.R., 2015. Papio Cranium from the Hominin-Bearing Site of Malapa: Implications for the Evolution of Modern Baboon Cranial Morphology and South African Plio-Pleistocene Biochronology. PLOS ONE. 10, e0133361.

Gould, S.J., n.d. Ontogeny and phylogeny. 1977. Cambridge. Belknap.

Grabowski, M., 2016. Bigger Brains Led to Bigger Bodies?: The Correlated Evolution of Human Brain and Body Size. Current Anthropology. 57, 174–196.

Girard, L., 1910. Essai d'anatomie topographique du labyrinthe d'après les dissections pratiquées par voie chirurgicale. Bull Mém Soc Anat. 85, 941–962.

Girard, L., 1923. Le plan des canaux semi-circulaires horizontaux considéré comme plan horizontal de la tête. Bulletin et Mémoires de la Societe d'Anthropologie de Paris. 14–33.Girard, L.-P., 1924. Rapport sur l'attribution du Prix Broca, en 1922 et 1924. Bulletins et Mémoires de la Société d'Anthropologie de Paris. 5, 93–94.

Girard, L.-P., 1929. Conférence Broca.—Lattitude normale de la tête déterminée par le labyrinthe de l'oreille. Bulletins et Mémoires de la Société d'Anthropologie de Paris. 10, 79–99.

Gommery, D., Sénégas, F., Thackeray, J.F., 2014. Cercopithecoidea material from the Middle Pliocene site, Waypoint 160, Bolt's Farm, South Africa. Annals of the Ditsong National Museum of Natural History. 4, 1–8.

González-Forero, M., Gardner, A., 2018. Inference of ecological and social drivers of human brain-size evolution. Nature. 557, 554–557

Gould, S.J., 1975. Allometry in primates, with emphasis on scaling and the evolution of the brain. Contributions to primatology. 5, 244–292.

Graf, W., 1988. Motion detection in physical space and its peripheral and central representation. Annals of the New York Academy of Sciences.

Grafen, A. and Hails, R., 2002. *Modern statistics for the life sciences*. Oxford University Press.

Grabowski, M., 2016. Bigger Brains Led to Bigger Bodies?: The Correlated Evolution of Human Brain and Body Size. Current Anthropology. 57, 174–196.

Granatosky, M.C., 2018. A Review of locomotor diversity in mammals with analyses exploring the influence of substrate use, body mass and intermembral index in primates. Journal of Zoology. 306, 207–216.

Green, D.J., Gordon, A.D., Richmond, B.G., 2007. Limb-size proportions in Australopithecus afarensis and Australopithecus africanus. Journal of Human Evolution. 52, 187–200.

Hall, K.R.L., 1960. Social Vigilance Behaviour of the Chacma Baboon, Papio Ursinus. Behaviour. 16, 261–293.

Halley, A.C., Deacon, T.W., 2017. 3.09 - The Developmental Basis of Evolutionary Trends in Primate Encephalization. In: Kaas, J.H. (Ed.), Evolution of Nervous Systems (Second Edition). Academic Press, Oxford, pp. 149–162.

Herculano-Houzel, S., Kaas, J.H., 2011. Gorilla and Orangutan Brains Conform to the Primate Cellular Scaling Rules: Implications for Human Evolution. Brain, Behavior and Evolution. 77, 33–44.

Howard, L.H., Lonsdorf, E.V., 2022. The Eyes Have It. Primate Cognitive Studies.

Hullar, T.E., 2006. Semicircular canal geometry, afferent sensitivity, and animal behavior. The Anatomical Record Part A: Discoveries in Molecular, Cellular, and Evolutionary Biology. 288A, 466–472.

Hunt, K.D., Cant, J.G.H., Gebo, D.L., Rose, M.D., Walker, S.E., Youlatos, D., 1996. Standardized descriptions of primate locomotor and postural modes. Primates. 37, 363–387.

Isler, K., Christopher Kirk, E., Miller, J.M.A., Albrecht, G.A., Gelvin, B.R., Martin, R.D., 2008a. Endocranial volumes of primate species: scaling analyses using a comprehensive and reliable data set. Journal of Human Evolution. 55, 967–978.

Isler, K., Christopher Kirk, E., Miller, J.M.A., Albrecht, G.A., Gelvin, B.R., Martin, R.D., 2008b. Endocranial volumes of primate species: scaling analyses using a comprehensive and reliable data set. Journal of Human Evolution. 55, 967–978.

Jaanusson, V., 1987. Balance of the head in hominid evolution. Lethaia. 20, 165–176.

Jeanmougin, F., Thompson, J.D., Gouy, M., Higgins, D.G. and Gibson, T.J., 1998. Multiple sequence alignment with Clustal X. *Trends in biochemical sciences*, *23*(10), pp.403-405.

Jeffery, N., Spoor, F., 2002. Brain size and the human cranial base: A prenatal perspective. American Journal of Physical Anthropology. 118, 324–340.

Jeffery, N., Spoor, F., 2006. The primate subarcuate fossa and its relationship to the semicircular canals part I: prenatal growth. Journal of Human Evolution. 51, 537–549.

Le Maître, A., 2019. Role of Spatial Integration in the Morphology of the Bony Labyrinth in Modern Humans. Bulletins et Mémoires de la Société d'Anthropologie de Paris. 31, 34–42.

Le Maître, A., Schuetz, P., Vignaud, P., Brunet, M., 2017. New data about semicircular canal morphology and locomotion in modern hominoids. Journal of Anatomy. 231, 95–109.

Lebedkin, S., 1924. Uber die Lage des Canalis semicircularis lateralis bei Saugern. Anatomischer Anzeiger. 58, 449–460.

Lebrun, R., Perier, A., Masters, J., Marivaux, L. and Couette, S., 2021. Lower levels of vestibular developmental stability in slow-moving than fast-moving primates. *Symmetry*, *13*(12), p.2305.

Lebrun, R., Godinot, M., Couette, S., Tafforeau, P., Zollikofer, C., 2012. The labyrinthine morphology of Pronycticebus gaudryi (Primates, Adapiformes). Palaeobiodiversity and Palaeoenvironments. 92, 527–537.

Lebrun, R., León, M.P.D., Tafforeau, P., Zollikofer, C., 2010. Deep evolutionary roots of strepsirrhine primate labyrinthine morphology. Journal of Anatomy. 216, 368–380.

Leigh, S.R., 2006. Cranial ontogeny of Papio baboons (Papio hamadryas). American Journal of Physical Anthropology. 130, 71–84.

Lesciotto, K.M., Richtsmeier, J.T., 2019. Craniofacial skeletal response to encephalization: How do we know what we think we know? American Journal of Physical Anthropology. 168 Suppl 67, 27–46.

Lieberman, D.E., 2011. 10 Sense and Sensitivity: Vision, Hearing, Olfaction, and Taste. In: The Evolution of the Human Head. Harvard University Press, pp. 374–413.

Lieberman, D.E., Hallgrímsson, B., Liu, W., Parsons, T.E., Jamniczky, H.A., 2008. Spatial packing, cranial base angulation, and craniofacial shape variation in the mammalian skull: testing a new model using mice. Journal of Anatomy. 212, 720–735.

Lieberman, D.E., McBratney, B.M., Krovitz, G., 2002. The evolution and development of cranial form in Homo sapiens. Proceedings of the National Academy of Sciences. 99, 1134–1139.

Lieberman, D.E., Ross, C.F., Ravosa, M.J., 2000. The primate cranial base: Ontogeny, function, and integration. American Journal of Physical Anthropology. 113, 117–169.

Luo, L., 2020. Principles of Neurobiology, 2nd ed. CRC - Taylor and Francis, Abingdon, Oxon.

Maier, W., 1977. Chronology and biology of the South African australopithecines. Journal of Human Evolution. 6, 89–93.

Malinzak, M.D., 2010. Experimental Analyses of the Relationship Between Semicircular Canal Morphology and Locomotor Head Rotations in Primates.

Malinzak, M.D., Kay, R.F., Hullar, T.E., 2012a. Locomotor head movements and semicircular canal morphology in primates. Proceedings of the National Academy of Sciences. 109, 17914–17919.

Malinzak, M.D., Kay, R.F., Hullar, T.E., 2012b. Locomotor head movements and semicircular canal morphology in primates. Proceedings of the National Academy of Sciences. 109, 17914–17919.

Marino, F.E., Sibson, B.E., Lieberman, D.E., 2022. The evolution of human fatigue resistance. Journal of Comparative Physiology B. 192, 411–422.

Marugán-Lobón, J., Chiappe, L.M., Farke, A.A., 2013. The variability of inner ear orientation in saurischian dinosaurs: testing the use of semicircular canals as a reference system for comparative anatomy. PeerJ. 1, e124.

McHenry, H.M., 1982. The pattern of human evolution: studies on bipedalism, mastication, and encephalization. Annual Review of Anthropology. 151–173.

McPhee, B.W., Benson, R.B., Botha-Brink, J., Bordy, E.M. and Choiniere, J.N., 2018. A giant dinosaur from the earliest Jurassic of South Africa and the transition to quadrupedality in early sauropodomorphs. *Current Biology*, *28*(19), pp.3143-3151.

Mooney, M.P., Siegel, M.I., Smith, T.D., Burrows, A.M., 2002. Evolutionary Changes in the Cranial Vault and Base: Establishing the Primate Form. In: Understanding Craniofacial Anomalies. John Wiley & Sons, Ltd, pp. 273–294.

Moss, M.L., 1958. Rotations of the cranial components in the growing rat and their experimental alteration. Acta Anatomica. 32, 65–86.

Morimoto, N., Morimoto, N., Kunimatsu, Y., Nakatsukasa, M., de León, M.S.P., Zollikofer, C.P.E., Ishida, H., Sasaki, T., Gen Suwa, 2020. Variation of bony labyrinthine morphology in Mio-Plio-Pleistocene and modern anthropoids. American Journal of Physical Anthropology. 173, 276–292.

Münkemüller, T., Lavergne, S., Bzeznik, B., Dray, S., Jombart, T., Schiffers, K., Thuiller, W., 2012. How to measure and test phylogenetic signal. Methods in Ecology and Evolution. 3, 743–756.

Muller, M., Verhagen, J.H.G., 2002. Optimization of the mechanical performance of a two-duct semicircular duct system—Part 3: the positioning of the ducts in the head. Journal of theoretical biology. 216, 443–459.

Mundry, R., 2014. Statistical issues and assumptions of phylogenetic generalized least squares, in: Modern Phylogenetic Comparative Methods and Their Application in Evolutionary Biology. Springer, pp. 131–153.

Napier, J.R., 1970. Paleoecology and catarrhine evolution. Old World monkeys: evolution, systematics, and behavior. 53–95.

Neaux, D., Wroe, S., Ledogar, J.A., Heins Ledogar, S., Sansalone, G., 2019. Morphological integration affects the evolution of midline cranial base, lateral basicranium, and face across primates. American Journal of Physical Anthropology. 170, 37–47.

Nett, E.M., Ravosa, M.J., 2019. Ontogeny of orbit orientation in primates. The Anatomical Record. 302, 2093–2104.

Nguyen, L.T., Schmidt, H.A., Von Haeseler, A. and Minh, B.Q., 2015. IQ-TREE: a fast and effective stochastic algorithm for estimating maximum-likelihood phylogenies. *Molecular biology and evolution*, *32*(1), pp.268-274.

Ni, X., Flynn, J.J., Wyss, A.R., Zhang, C., 2019. Cranial endocast of a stem platyrrhine primate and ancestral brain conditions in anthropoids. Science Advances. 5, eaav7913.

Pagel, M., 1999. Inferring the historical patterns of biological evolution. Nature. 401, 877–884.

Pagel, M., 2002. Modelling the evolution of continuously varying characters on phylogenetic trees. Morphology, shape and phylogeny. 269, 286.

Paradis, E., Claude, J. and Strimmer, K., 2004. APE: analyses of phylogenetics and evolution in R language. *Bioinformatics*, *20*(2), pp.289-290.

Pereira-Pedro, A.S., Bruner, E., 2022. Craniofacial orientation and parietal bone morphology in adult modern humans. Journal of Anatomy. 240, 330–338.

Perez, F., 1922. Crâniologie vestibienne, ethnique et zoologique. Bulletins et Mémoires de la Société d'Anthropologie de Paris. 3, 16–32.

Plomp, K.A., Dobney, K., Collard, M., 2020. Spondylolysis and spinal adaptations for bipedalism: The overshoot hypothesis. Evolution, Medicine, and Public Health. 2020, 35–44.

Potts, R., 1998a. Variability selection in hominid evolution. Evolutionary Anthropology: Issues, News, and Reviews: Issues, News, and Reviews. 7, 81–96.

Potts, R., 1998b. Environmental hypotheses of hominin evolution. American Journal of Physical Anthropology. 107, 93–136.

Powell, L.E., Isler, K., Barton, R.A., 2017. Re-evaluating the link between brain size and behavioural ecology in primates. Proceedings of the Royal Society B: Biological Sciences. 284, 20171765.

Pregibon, A., Williams, F., 2021. Examining the Dietary Behavior of Australopithecus robustus and Rossil Primates from Swartkrans, South Africa Using Low-Magnification Stereomicroscopy of Dental Microwear. Georgia Journal of Science. 79.

Preuschoft, H., Franzen, J.L., 2012. Locomotion and biomechanics in Eocene mammals from Messel. Palaeobiodiversity and Palaeoenvironments. 92, 459–476.

Pugh, K.D., Gilbert, C.C., 2018. Phylogenetic relationships of living and fossil African papionins: Combined evidence from morphology and molecules. Journal of Human Evolution. 123, 35–51.

Purves, D., Augustine, G.J., Fitzpatrick, D., Hall, W.C., Lamantia, A.S., Mooney, R.D., Platt, M.L., White, L.E., 2018. The Vestibular System. In: Neuroscience. Oxford University Press, New York, pp. 305–320.

R Core Team, 2022. R: A Language and Environment for Statistical Computing.

Raichlen, D.A., Pontzer, H., 2021. Energetic and endurance constraints on great ape quadrupedalism and the benefits of hominin bipedalism. Evolutionary Anthropology: Issues, News, and Reviews. 30, 253–261.

Rasband, W.S., 1997. ImageJ. Bethesda, MD.

Revell, L.J., Harmon, L.J., Collar, D.C., 2008. Phylogenetic Signal, Evolutionary Process, and Rate. Systematic Biology. 57, 591–601.

Revell, L.J., 2012. phytools: an R package for phylogenetic comparative biology (and other things). Methods in ecology and evolution. 3, 217–223.

Rollinson, J., 1981. Comparative aspects of primate locomotion, with special reference to arboreal cercopithecines. Presented at the Symp. Zool. Soc. Lond., pp. 377–427.

Ronquist, F., Teslenko, M., Van Der Mark, P., Ayres, D.L., Darling, A., Höhna, S., Larget, B., Liu, L., Suchard, M.A., Huelsenbeck, J.P., 2012. MrBayes 3.2: efficient Bayesian phylogenetic inference and model choice across a large model space. Systematic biology. 61, 539–542.

Ross, C.F., Ravosa, M.J., 1993. Basicranial flexion, relative brain size, and facial kyphosis in nonhuman primates. American Journal of Physical Anthropology. 91, 305–324.

Ross, C.F., Henneberg, M., 1995. Basicranial flexion, relative brain size, and facial kyphosis in Homo sapiens and some fossil hominids. American Journal of Physical Anthropology. 98, 575–593.

Ryan, T.M., Silcox, M.T., Walker, A., Mao, X., Begun, D.R., Benefit, B.R., Gingerich, P.D., Köhler, M., Kordos, L., McCrossin, M.L., Moyà-Solà, S., Sanders, W.J., Seiffert, E.R., Simons, E.L., Zalmout, I.S., Spoor, F., 2012. Evolution of locomotion in Anthropoidea: the semicircular canal evidence. Proceedings of The Royal Society B: Biological Sciences. 279, 3467–3475.

Ruff, C. B., Trinkaus, E., & Holliday, T. W., 1997. Body massand encephalization in Pleistocene Homo. Nature, 387, 173–176.

Ryan, T.M., Carlson, K.J., Gordon, A.D., Jablonski, N., Shaw, C.N., Stock, J.T., 2018. Human-like hip joint loading in Australopithecus africanus and Paranthropus robustus. Journal of Human Evolution. 121, 12–24.

Sansalone, G., Allen, K., Ledogar, J.A., Ledogar, S., Mitchell, D.R., Profico, A., Castiglione, S., Melchionna, M., Serio, C., Mondanaro, A., Raia, P., Wroe, S., 2020. Variation in the strength of allometry drives rates of evolution in primate brain shape. Proceedings of the Royal Society B: Biological Sciences. 287, 20200807.

Sawaguchi, T., 1990. Relative brain size, stratification, and social structure in anthropoids. Primates. 31, 257–272.

Sanders, R.K., Smith, D.K., 2005. The endocranium of the theropod dinosaur Ceratosaurus studied with computer tomography. Acta Palaeontologica Polonica. 50

Schaefer, K., Mitteroecker, P., Gunz, P., Bernhard, M. and Bookstein, F.L., 2004. Craniofacial sexual dimorphism patterns and allometry among extant hominids. Annals of Anatomy-Anatomischer Anzeiger, 186(5-6), pp.471-478.

Schade, M., Rauhut, O.W.M., Evers, S.W., 2020. Neuroanatomy of the spinosaurid Irritator challengeri (Dinosauria: Theropoda) indicates potential adaptations for piscivory. Scientific Reports. 10, 9259.

Schellhorn, R., 2018. A potential link between lateral semicircular canal orientation, head posture, and dietary habits in extant rhinos (Perissodactyla, Rhinocerotidae). Journal of Morphology. 279, 50–61.

Schloerke, B., Cook, D., Larmarange, J., Briatte, F., Marbach, M., Thoen, E., Elberg, A., Toomet, O., Crowley, J., Hofmann, H., Wickham, H., 2021. GGally: Extension to “ggplot2.”

Schmitt, D., 2010. Primate locomotor evolution: Biomechanical studies of primate locomotion and their implications for understanding primate neuroethology. Primate neuroethology. 10–30.

Schoenemann, A., 1906. Schläfenbein und Schädelbasis, eine anatomisch-otiatrische Studie. Gesellsch.

Schoenemann, P.T., 2013. Hominid brain evolution. A companion to paleoanthropology. 136–164.

Shannon, C.E., 1949. The Mathematical Theory of Communication by CE Shannon and W. Weaver.

Singleton, M., 2012. Postnatal cranial development in papionin primates: an alternative model for hominin evolutionary development. Evolutionary Biology, 39(4), pp.499-520.

Singleton, M., Seitelman, B.C., Krecioch, J.R. and Frost, S.R., 2017. Cranial sexual dimorphism in the Kinda baboon (Papio hamadryas kindae). American Journal of Physical Anthropology, 164(4), pp.665-678.

Spoor, F., 1997. Basicranial architecture and relative brain size of Sts 5. South African journal of science. 93, 182–18.

Spoor, F., 2003. The semicircular canal system and locomotor behaviour, with special reference to hominin evolution. Courier-Forschungsinstitut Senckenberg. 93–104

Spoor, F., Wood, B., Zonneveld, F., 1994. Implications of early hominid labyrinthine morphology for evolution of human bipedal locomotion. Nature. 369, 645–648.

Spoor, F., 1997. Basicranial architecture and relative brain size of Sts 5. South African journal of science. 93, 182–1.

Spoor, F., Zonneveld, F., 1998. Comparative review of the human bony labyrinth. American Journal of Physical Anthropology: The Official Publication of the American Association of Physical Anthropologists. 107, 211–251.

Strait, D.S., Ross, C.F., 1999. Kinematic data on primate head and neck posture: implications for the evolution of basicranial flexion and an evaluation of registration planes used in palaeoanthropology. American Journal of Physical Anthropology: The Official Publication of the American Association of Physical Anthropologists. 108, 205–222.

Strasser, E., 1988. Pedal evidence for the origin and diversification of cercopithecoid clades. Journal of Human Evolution. 17, 225–245.

Taylor, M.P., Wedel, M.J., Naish, D., 2009. Head and neck posture in sauropod dinosaurs inferred from extant animals. Acta Palaeontologica Polonica. 54, 213–220.

Thackeray, F.J., Dumoncel, J., Gommery, D., Kgasi, L., Tawane, G.M., de Beer, F.C., Hoffman, J.W., Bam, L.C., 2019. Morphometric comparison of semicircular canals of Parapapio broomi and P. jonesi from Sterkfontein, South Africa. South African Journal of Science. 115, 1–3.

Urciuoli, A., Zanolli, C., Beaudet, A., Dumoncel, J., Santos, F., Moyà-Solà, S., Alba, D.M., 2020. The evolution of the vestibular apparatus in apes and humans. eLife. 9, e51261.

Urciuoli, A., 2021. The evolution of semicircular canals in anthropoid primates : Phylogenetic implications for Miocene catarrhines. Universitat Autònoma de Barcelona. Programa de Doctorat en Biodiversitat.

Van Der Klaauw, C.J., 1952. Size and position of the functional components of the skull. A contribution to the knowledge of the architecture of the skull, based on data in the literature. Archives Néerlandaises de Zoologie. 9, 1–556.

Vanderpool, D., Minh, B.Q., Lanfear, R., Hughes, D., Murali, S., Harris, R.A., Raveendran, M., Muzny, D.M., Hibbins, M.S., Williamson, R.J. and Gibbs, R.A., 2020. Primate phylogenomics uncovers multiple rapid radiations and ancient interspecific introgression. PLoS biology, 18(12), p.e3000954.

Van Woerden, J.T., Van Schaik, C.P., Isler, K., 2010. Effects of seasonality on brain size evolution: evidence from strepsirrhine primates. The American Naturalist. 176, 758–767.

Vidal, P.P., Graf, W., Berthoz, A., 1986. The orientation of the cervical vertebral column in unrestrained awake animals. Experimental Brain Research. 61, 549–559.

White, T.D. Black, M. Folkens, P.A., 2012. Chapter 4: Skull: Cranium and Mandible. In: Human osteology. 3rd Edition. Academic Press, Elsevier, Burlington, USA, , pp. 43 – 10.

Vrba, E.S., 1985. Ecological and adaptive changes associated with early hominid evolution. Ancestors: The hard evidence. 63–71.

Ward, C.V., Kimbel, W.H., Johanson, D.C., 2011. Complete Fourth Metatarsal and Arches in the Foot of Australopithecus afarensis. Science. 331, 750–753.

Walker, A., Ryan, T.M., Silcox, M.T., Simons, E.L., Spoor, F., 2008. The semicircular canal system and locomotion: the case of extinct lemuroids and lorisoids. Evolutionary Anthropology: Issues, News, and Reviews: Issues, News, and Reviews. 17, 135–145.

Ward, C.V., 2013. Postural and locomotor adaptations of Australopithecus species. In: The Paleobiology of Australopithecus. Springer, pp. 235–245.

McHenry, H.M., Berger, L.R., 1998. Body proportions in Australopithecus afarensis and A. africanus and the origin of the genus Homo. Journal of Human Evolution. 35, 1–22.

McNutt, E.J., Zipfel, B., DeSilva, J.M., 2018. The evolution of the human foot. Evolutionary Anthropology: Issues, News, and Reviews. 27, 197–217.

Werner, C., 1933. Das Ohrlabyrinth der Tiere. PassowScha ¨fer Beitr. 30, 390–408.

Wickham, H., Chang, W., Wickham, M.H., 2016. Package ‘ggplot2.’ Create elegant data visualisations using the grammar of graphics. Version. 2, 1–189.

Williams, F. l., Ackermann, R. r., Leigh, S. r., 2007. Inferring Plio-Pleistocene southern African biochronology from facial affinities in Parapapio and other fossil papionins. American Journal of Physical Anthropology. 132, 163–174.

Witmer, L.M., Ridgely, R.C., Dufeau, D.L., Semones, M.C., 2008. Using CT to Peer into the Past: 3D Visualization of the Brain and Ear Regions of Birds, Crocodiles, and Nonavian Dinosaurs. In: Endo, H., Frey, R. (Eds.), Anatomical Imaging: Towards a New Morphology. Springer Japan, Tokyo, pp. 67–87.

Wolpoff, M.H., 1981. Cranial capacity estimates for Olduvai Hominid 7. American Journal of Physical Anthropology. 56, 297–304.

Zipfel, B., DeSilva, J.M., Kidd, R.S., Carlson, K.J., Churchill, S.E., Berger, L.R., 2011. The Foot and Ankle of Australopithecus sediba. Science. 333, 1417–1420.

Zollikofer, C.P.E., De León, M.S.P., 2013. Pandora's growing box: inferring the evolution and development of hominin brains from endocasts. Evolutionary Anthropology: Issues, News, and Reviews. 22, 20–33.